

Chapter 3

Formulation of Equivalent Frame

Model with Deformable Connectors

3.1 Introduction

This chapter introduces the formulation of a new computationally efficient modelling approach named ‘equivalent frame model with deformable connectors’ (shortened as ‘EQFdc model’) to be used in tunnelling-induced damage assessment of masonry buildings. This approach idealises the building as an equivalent frame by using beam elements to model piers and spandrels, similar to the concept used in the earthquake engineering field. However, instead of defining the connections between the piers and spandrels as rigid, deformable connectors are used, which are modelled with 2D macro-elements. Macro-elements are intended to eliminate the overestimation of building stiffness caused by the rigid sections defined in the original equivalent frame modelling approach (Section 2.4.1.3). Although macro-elements alone are sufficient to determine the overall building response in tunnel-soil-structure interaction problems, beam elements have some advantages in capturing strain distributions and accounting for material nonlinearity. Consequently, they are utilised alongside macro-elements.

3.2 Preliminary Work

Preliminary work conducted on the development of the equivalent frame model with rigid connectors (EQF model) and the macro-element model is briefly presented in this section. The EQF and macro-element modelling approaches are mostly employed for the seismic assessment of masonry buildings in the literature but they were used to address tunnelling-induced damage assessment of masonry buildings for the first time in this research. The EQF and 2D macro-element models are assessed with linear elastic analysis, considering it as an initial step of the damage assessment procedure. The soil-structure interactions in the EQF and the 2D macro-element models are provided by a 1D FE Winkler soil-foundation model, where the greenfield displacements are computed by the empirical equations. Building responses determined from the EQF and the macro-element models are compared with the results obtained from a 2D FE continuum model. The outcomes of the preliminary work provide a basis for the development of the EQFdc modelling approach, which is explained in the following sections in detail.

3.2.1 Equivalent frame model with rigid connectors

To idealise the masonry façade according to the EQF model, the TREMURI approach (Figures 2.9 and 2.10e) was adopted from Lagomarsino et al. (2013), considering the layout of the façade openings. Figure 3.1 shows the EQF model idealisation of a two-storey masonry building in terms of spandrels, piers and rigid connectors and its interaction with the soil elements through the 1D FE Winkler soil-foundation model. The FE formulations employed for the EQF model are presented in detail by Gulen et al. (2021). Soil-structure interaction analyses were carried out using the EQF model. The EQF model demonstrated stiffer response than the 2D FE continuum model due to the presence of the rigid connector elements (Gulen et al., 2021).

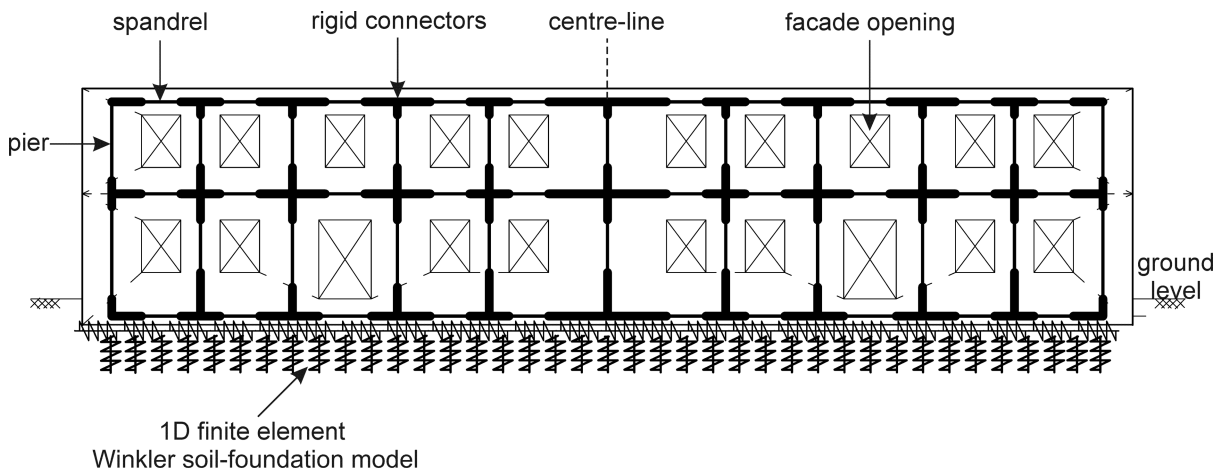


Figure 3.1: Equivalent frame model with rigid connectors (Gulen et al., 2021).

3.2.2 Macro-element model

After encountering a stiffer response (compared to the 2D FE continuum model) in the EQF model due to the rigid connectors, a macro-element model is developed in 2D. A macro-element comprises a 4-noded quadrilateral (referred to as ‘quad’) element with surrounding interfaces. The macro-element modelling approach idealises the masonry building in terms of macro-elements based on the layout of the façade openings without requiring the identification of beam elements and rigid connections. Masonry sections between the façade openings are modelled by the macro-elements (Caliò et al., 2012). Figure 3.2 shows the macro-element idealisation of a masonry building (same in Figure 3.1) with coarse (Figure 3.2a) and fine (Figure 3.2b) mesh discretisation options.

The formulations developed for the macro-element model in this research are different from those developed by Caliò et al. (2012). Caliò et al. (2012) used discrete element-based formulations, whereas finite element formulations are developed in this study. Additionally, the choice of degrees of freedom (DOF) formulated in this macro-element model is completely different from the ones used by Caliò et al. (2012). The formulations used in the macro-element model are presented by Gulen et al. (2022) in detail.

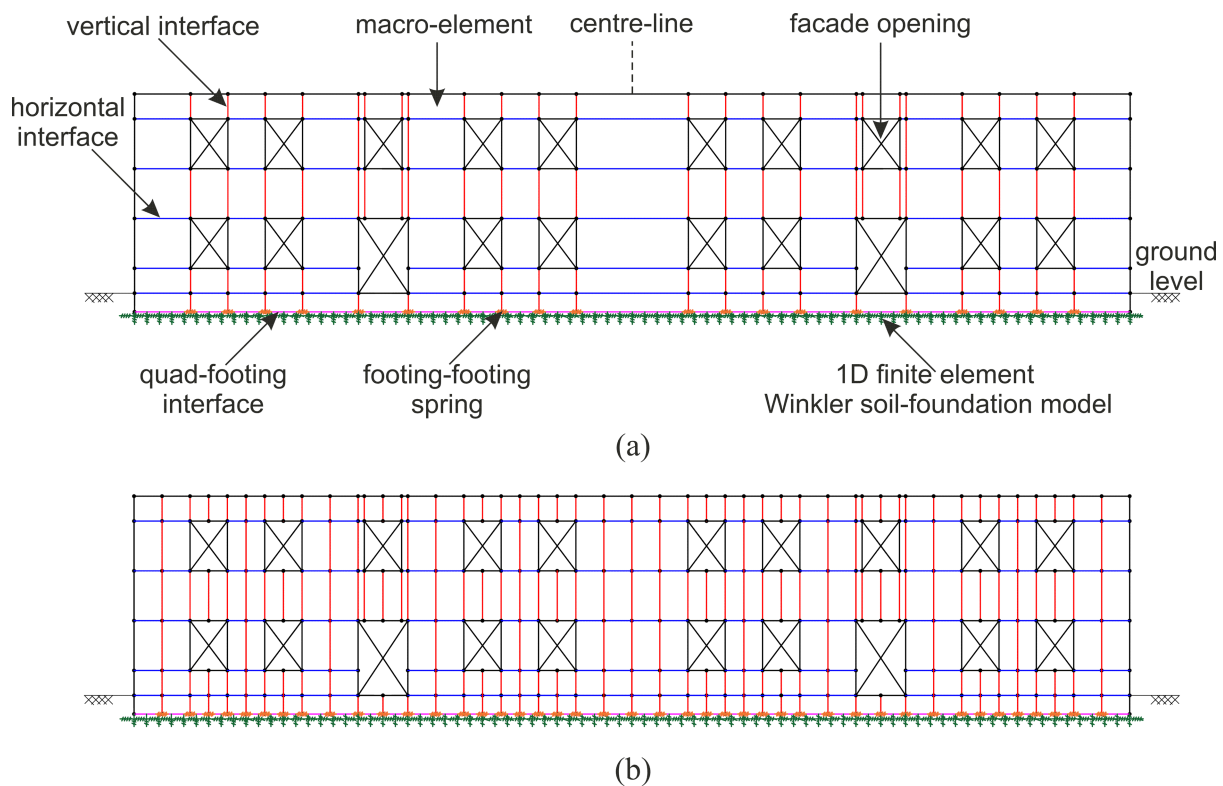


Figure 3.2: The 2D macro-element model idealisation of a masonry façade: (a) coarse mesh, (b) fine mesh (Gulen et al., 2022).

In this macro-element model, a novel approach is presented to model the interaction between the building and the foundation (Figure 3.16), which is neglected in the existing macro-element models available in the literature. Another advantage of the developed macro-element model is that it enables the calculation of strains inside the macro-element (Section 3.6.1) for tunnelling-induced damage assessment purposes.

According to linear elastic analysis comparisons, the building displacements determined from the macro-element models presented good agreements with the 2D FE continuum model, even for the coarse mesh model. For the comparison of the major principal tensile strain distributions, using a finer mesh (Figure 3.2b) of macro-elements captures the strain distributions in the building slightly better than the coarse mesh model (Figure 3.2a) compared to the 2D FE continuum model. However, to capture the bending and shear stress distributions in the element axis and cross-sections accurately, it is concluded that implementing the beam

behaviour directly to the building model is more practical than using a fine mesh macro-element model.

3.3 EQFdc Model Overview

The EQFdc modelling approach aims to combine the advantageous features of both EQF and macro-element models in one model, which can formulate the beam behaviour directly as in the EQF model but eliminate the overestimation of façade stiffness induced by the rigid connectors by replacing them with deformable macro-elements as in the macro-element model.

The EQFdc modelling concept for a simple building example is shown in Figure 3.3. In the EQFdc model idealisation, the element geometries are determined according to the layout of adjacent façade openings. The pier and spandrel elements of the building are defined using the full rigid offset method (Figure 2.10c) proposed by Bracchi et al. (2015). Flexibility-based Timoshenko beam element formulations are used to model the spandrels and piers. These formulations are different from the ones developed for spandrel and pier elements in the EQF model (i.e. with rigid connectors), which are based on conventional stiffness-based FE formulations. Using flexibility-based FE formulations provides advantages for the nonlinear constitutive model implementations. The nonlinear constitutive models used for the structural elements in this thesis are formulated from 1D stress-strain relationships (Iwan, 1967). Since the flexibility-based FE formulations are based on force-equilibrium equations instead of displacement-based equations (i.e. used for the conventional stiffness-based FE formulations), the 1D stress-strain based constitutive models can be practically implemented into the EQFdc model from the element and Gauss point level iterations (explained in Chapters 4 and 6).

The masonry sections, where spandrels are connected to piers (Figure 3.3), are modelled with deformable macro-elements (referred to as ‘deformable connectors’). Each macro-element interacts with adjacent quad, beam or footing elements via zero-thickness structural interface

elements (Figures 3.3b and 3.3c). The formulation of the macro-elements is based on the preliminary work (Gulen et al., 2022).

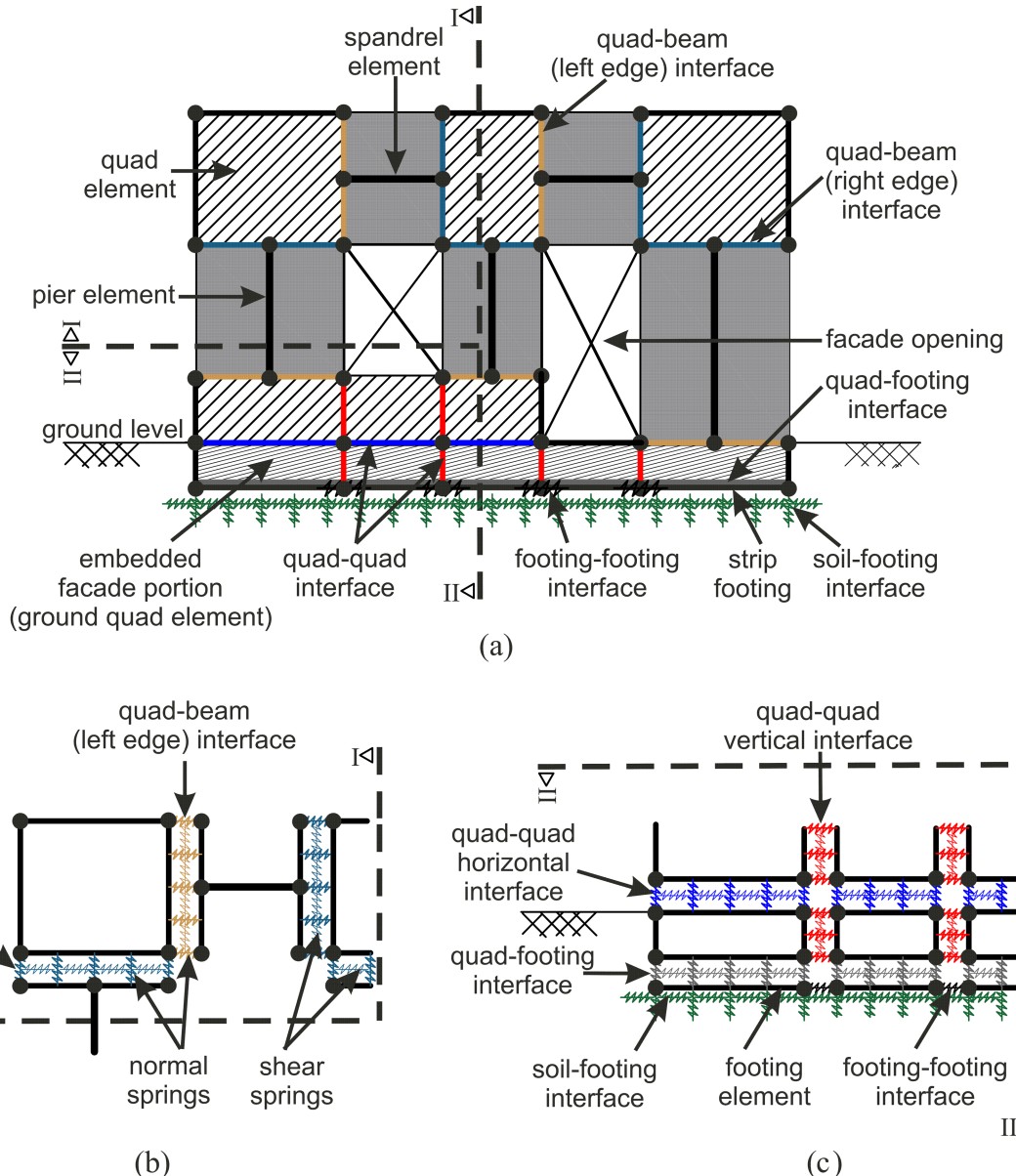


Figure 3.3: EQFdc modelling approach: (a) EQFdc discretisation of a simple building, (b) quad-beam interface representation, (c) quad-quad, quad-footing and soil-foundation interface representations.

The masonry portions interacting with the footing elements below the ground level are also modelled with macro-elements (Figure 3.3c). The soil-structure interaction is modelled using the S2M soil-foundation interaction model (Section 2.5.2.1). Rigid footing elements are modelled between the soil-foundation interaction model and the macro-elements. These

footing elements ensure displacement compatibility between soil-footing interface and macro-elements through rigid bar elements but incorporate the axial deformability of foundations by placing axial springs between the rigid bar elements (Figure 3.3c). The axial stiffness of the footings is lumped in axial springs (footing-footing interface in Figure 3.3c).

Tunnelling-induced greenfield displacements are applied to the EQFdc model from the soil-footing interface elements (Figure 3.3c) as prescribed deformations.

The finite element formulations developed in this chapter are based on the virtual work form of the governing equations. Small deformations are assumed and infinitesimal strains are considered. Vectors and matrices are written in bold type. Formulations presented in this chapter form a basis for the further implementations of the EQFdc model into linear and nonlinear models, explained in the following chapters.

3.4 Formulation of Flexibility-Based Elements

2D flexibility-based formulations are employed to model beam elements in the EQFdc model. The flexibility-based formulations presented in this chapter comprising axial and bending behaviour of the beam elements are based on those developed for the Euler-Bernoulli beam element by Spacone et al. (1996). However, the formulations are modified to include the shear terms. The contribution of shear is included in the flexibility formulations with additional terms placed into the force interpolation functions, the section forces and the section flexibility matrix (Martino et al., 2000; Marini & Spacone, 2006).

3.4.1 Global and reduced degrees of freedom

The beam element formulations are derived according to Timoshenko beam theory with constant shear strain. In Timoshenko beam theory, the cross-section of the beam remains plane. However, the beam experiences a constant shear strain, γ_0 , in addition to the rotation of the

neutral axis of the beam, $\frac{dv}{dx}$ (where v is the vertical displacement) and the rotation of the beam cross-section, θ .

$$u = u_c - y\theta \quad (3.1)$$

where u is the horizontal displacement in the beam element, u_c is the axial displacement at the element centroid and y is the distance from the element centroid along the beam cross-section. Accordingly, the shear strain and the relationship with the cross-section rotation are:

$$\gamma_0 = \frac{du}{dy} + \frac{dv}{dx} \quad \theta = \frac{dv}{dx} - \gamma_0 \quad (3.2)$$

The single beam element defined in the local member coordinate system is shown in Figure 3.4, where the nodal degrees of freedom vector, $\mathbf{U}_{\text{beam}}^*$ and the corresponding element nodal forces, $\mathbf{P}_{\text{beam}}^*$, are represented as:

$$\mathbf{U}_{\text{beam}}^* = [U_1^* \quad V_1^* \quad \theta_1^* \quad U_2^* \quad V_2^* \quad \theta_2^*]^T \quad (3.3)$$

$$\mathbf{P}_{\text{beam}}^* = [F_{x1}^* \quad F_{y1}^* \quad M_1^* \quad F_{x2}^* \quad F_{y2}^* \quad M_2^*]^T \quad (3.4)$$

Accordingly, the nodal degrees of freedom vector, \mathbf{U}_{beam} and corresponding element nodal forces, \mathbf{P}_{beam} , in the global coordinate system are defined as:

$$\mathbf{U}_{\text{beam}} = [U_1 \quad V_1 \quad \theta_1 \quad U_2 \quad V_2 \quad \theta_2]^T \quad (3.5)$$

$$\mathbf{P}_{\text{beam}} = [F_{x1} \quad F_{y1} \quad M_1 \quad F_{x2} \quad F_{y2} \quad M_2]^T \quad (3.6)$$

The nodal degrees of freedom and forces in the global coordinates system are transformed to the vectors in the local coordinates by the rotation matrix, \mathbf{R} :

$$\mathbf{U}_{\text{beam}}^* = \mathbf{R} \mathbf{U}_{\text{beam}} \quad \mathbf{P}_{\text{beam}}^* = \mathbf{R} \mathbf{P}_{\text{beam}} \quad (3.7)$$

$$\mathbf{R} = \begin{bmatrix} c & s & 0 & 0 & 0 & 0 \\ -s & c & 0 & 0 & 0 & 0 \\ 0 & 0 & 1 & 0 & 0 & 0 \\ 0 & 0 & 0 & c & s & 0 \\ 0 & 0 & 0 & -s & c & 0 \\ 0 & 0 & 0 & 0 & 0 & 1 \end{bmatrix} \quad (3.8)$$

where $c = \cos\theta$ and $s = \sin\theta$ and θ is the (anti-clockwise) angle of rotation from the global coordinates to member coordinates (Figure 3.5).

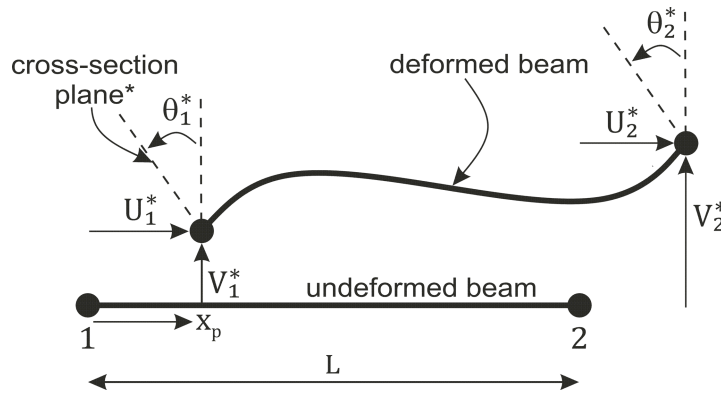


Figure 3.4: A finite beam element showing the degrees of freedom in member coordinates.

The global degrees of freedom vector includes three rigid body modes. To formulate the flexibility formulations, the reduced degrees of freedom need to be used (Spacone et al., 1996; Neuenhofer & Filippou, 1997). The displacement and force vectors generated by removing the rigid body modes are defined as reduced sets of displacements, \mathbf{U}_r , and forces, \mathbf{P}_r (Figure 3.6). The reduced set of displacements comprises the relative axial displacement, U_r , the rotation of node-1 relative to node-2, θ_{1r} and the rotation of node-2 relative to node-1, θ_{2r} .

$$\mathbf{U}_r = [U_r \quad \theta_{1r} \quad \theta_{2r}]^T \quad (3.9)$$

$$U_r = U_2^* - U_1^* \quad \theta_{1r} = \theta_1^* - \left(\frac{V_2^* - V_1^*}{L} \right) \quad \theta_{2r} = \theta_2^* - \left(\frac{V_2^* - V_1^*}{L} \right) \quad (3.10)$$

The reduced set of displacements vector is related to the degrees of freedom vector in the local coordinates by a reduced transformation matrix, \mathbf{T}_r .

$$\mathbf{U}_r = \mathbf{T}_r \mathbf{U}_{\text{beam}}^* \quad (3.11)$$

where \mathbf{T}_r is,

$$\mathbf{T}_r = \begin{bmatrix} -1 & 0 & 0 & 1 & 0 & 0 \\ 0 & 1/L & 1 & 0 & -1/L & 0 \\ 0 & 1/L & 0 & 0 & -1/L & 1 \end{bmatrix} \quad (3.12)$$

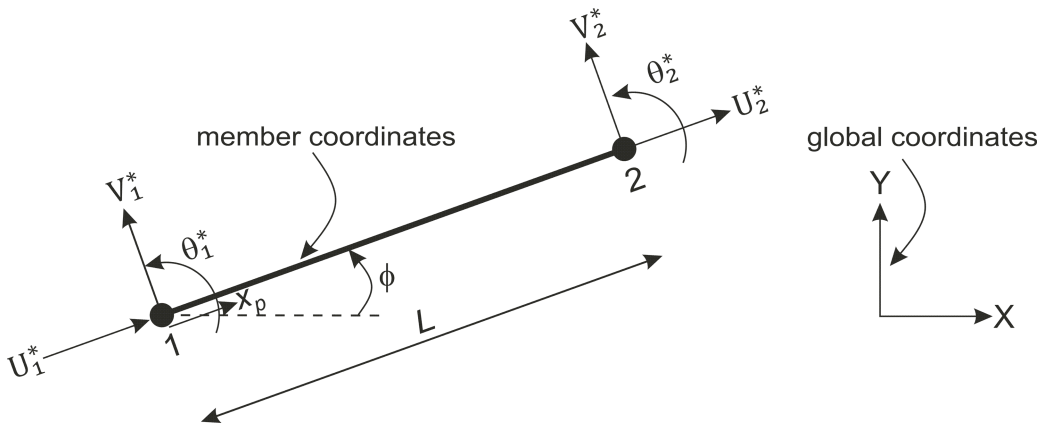


Figure 3.5: A finite beam element showing member and global coordinates.

The nodal forces satisfy three independent equilibrium equations based on horizontal force and moment equilibrium for a reduced, simply supported beam element. It is convenient to derive the reduced set of forces, \mathbf{P}_r , in terms of axial force (N) and bending moments (M_1 and M_2) at the element nodes.

$$\mathbf{P}_r = [N \quad M_1 \quad M_2]^T \quad (3.13)$$

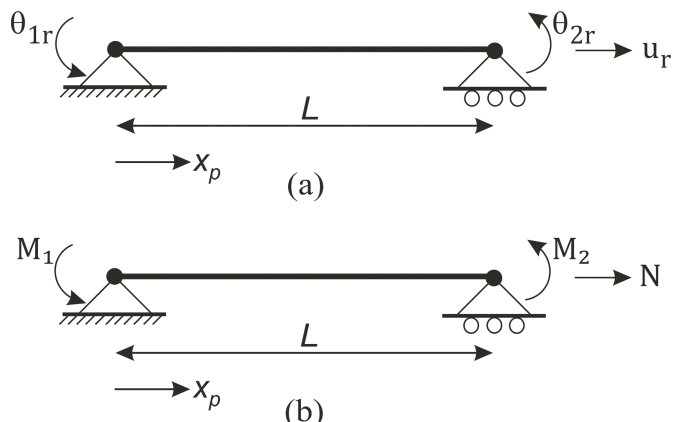


Figure 3.6: Beam element without rigid body modes showing a reduced set of: (a) displacements, \mathbf{U}_r and (b) forces, \mathbf{P}_r (modified from Marini & Spacone, 2006).

3.4.2 Virtual work for a single-beam element

The flexibility-based virtual work equations are derived for a single beam element with a length of L , based on Timoshenko beam theory with six degrees of freedom (Marini & Spacone, 2006). The internal and external virtual work equilibrium is written for a set of virtual forces, $\delta\mathbf{P}_{\text{beam}}$ applied to the beam element as:

$$(\delta\mathbf{P}_{\text{beam}})^T \mathbf{U}_{\text{beam}} = (\delta\mathbf{P}_r)^T \mathbf{U}_r = \int_0^L \int_0^{\text{Area}} (\delta\sigma \varepsilon dA) dx + \int_0^L \delta V \gamma dx \quad (3.14)$$

where $\delta\sigma$ is the virtual axial stress and ε is the axial strain in the infinitesimal cross-section area, dA . The axial strain, ε is defined in terms of the axial strain in the centroid of the beam cross-section, ε_c and the curvature, κ at distance, y , from the centroid as $\varepsilon = (\varepsilon_c + \kappa y)$.

The second term of internal virtual work represents the shear behaviour, where V and γ are the shear force and shear strain in the beam cross-section. The internal virtual work expression can be written in the open form of the section forces and deformations as follows:

$$\int_0^L \int_0^{\text{Area}} (\delta\sigma \varepsilon_c + \delta\sigma \kappa y) dA dx + \int_0^L \delta V \gamma dx = \int_0^L (\delta N \varepsilon_c + \delta M \kappa + \delta V \gamma) dx \quad (3.15)$$

The relationship between the section forces and the deformations can be summarised in a compact form of a set of internal stress resultants, \mathbf{p} and strain resultants, $\boldsymbol{\varepsilon}$ vectors as (Figure 3.7):

$$\int_0^L (\delta N \varepsilon_c + \delta M \kappa + \delta V \gamma) dx = \int_0^L \delta \mathbf{p}^T \boldsymbol{\varepsilon} dx \quad (3.16)$$

$$\mathbf{p} = [N \quad M \quad V]^T \quad \boldsymbol{\varepsilon} = [\varepsilon_c \quad \kappa \quad \gamma]^T \quad (3.17)$$

Here, it is convenient to determine the internal stress resultants vector from the reduced forces vector through the force interpolation functions, \mathbf{b} :

$$\mathbf{p} = \mathbf{b} \mathbf{P}_r \quad (3.18)$$

$$\mathbf{b} = \begin{bmatrix} 1 & 0 & 0 \\ 0 & \alpha - 1 & \alpha \\ 0 & -1/L & -1/L \end{bmatrix} \quad (3.19)$$

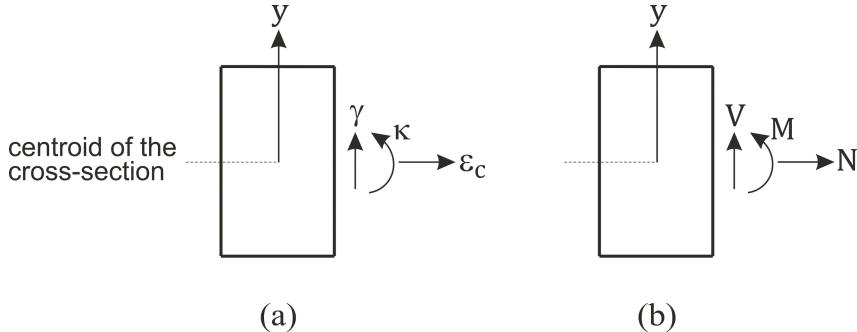


Figure 3.7: Beam cross-section level: (a) internal strain resultants, $\boldsymbol{\epsilon}$ and (b) internal stress resultants, \mathbf{p} (modified from Marini & Spacone, 2006).

where $\alpha = x_p/L$ for any position of the Gauss point. Accordingly, substituting Equation (3.18) into (3.16) and (3.14) gives the relationship between the reduced displacements and the section deformations as summarised:

$$(\delta\mathbf{P}_r)^T \mathbf{U}_r = \int_0^L (\delta\mathbf{P}_r)^T \mathbf{b}^T \boldsymbol{\epsilon} dx \quad (3.20)$$

Since $\delta\mathbf{P}_r$ is arbitrary, this gives,

$$\mathbf{U}_r = \int_0^L \mathbf{b}^T \boldsymbol{\epsilon} dx \quad (3.21)$$

The nodal forces in the global coordinates, \mathbf{P}_{beam} , can also be expressed in terms of a reduced set of forces, \mathbf{P}_r , as:

$$\mathbf{P}_{beam} = \mathbf{R}^T \mathbf{T}_r^T \mathbf{P}_r \quad (3.22)$$

3.4.3 Flexibility and stiffness matrices

The section deformations, $\boldsymbol{\epsilon}$ are related to the section forces, \mathbf{p} through the local flexibility matrix, \mathbf{f} as:

$$\boldsymbol{\epsilon} = \mathbf{f} \mathbf{p} \quad (3.23)$$

where the local flexibility matrix can be determined according to the material constitutive relationship as $\mathbf{f} = \left(\frac{\partial \boldsymbol{\epsilon}}{\partial \mathbf{p}} \right)$. Substituting Equations (3.23) and (3.18) into (3.21) gives the relationship between the reduced displacements, \mathbf{U}_r and the reduced forces, \mathbf{P}_r , as:

$$\mathbf{U}_r = \int_0^L \mathbf{b}^T \left(\frac{\partial \boldsymbol{\epsilon}}{\partial \mathbf{p}} \right) \mathbf{b} \mathbf{P}_r dx \quad (3.24)$$

The element flexibility matrix in the local coordinates, \mathbf{F} , is determined as:

$$\mathbf{F} = \int_0^L \mathbf{b}^T \left(\frac{\partial \boldsymbol{\epsilon}}{\partial \mathbf{p}} \right) \mathbf{b} dx \quad (3.25)$$

The relationship between the reduced displacements, \mathbf{U}_r and the reduced forces, \mathbf{P}_r , can be expressed using the element flexibility matrix, \mathbf{F} , as:

$$\mathbf{U}_r = \mathbf{F} \mathbf{P}_r \quad \mathbf{P}_r = \mathbf{F}^{-1} \mathbf{U}_r \quad (3.26)$$

Accordingly, substituting Equations (3.26), (3.11) and (3.7) into (3.22) gives the relationship between the nodal force, \mathbf{P}_{beam} and the nodal displacement vectors, \mathbf{U}_{beam} , in the global coordinates as:

$$\mathbf{P}_{beam} = \mathbf{R}^T \mathbf{T}_r^T \mathbf{F}^{-1} \mathbf{T}_r \mathbf{R} \mathbf{U}_{beam} \quad (3.27)$$

The element stiffness matrix in the global coordinates, \mathbf{K}_{beam} , is determined as:

$$\mathbf{K}_{beam} = \mathbf{R}^T \mathbf{T}_r^T \mathbf{F}^{-1} \mathbf{T}_r \mathbf{R} \quad (3.28)$$

\mathbf{K}_{beam} matrix can be directly assembled into the global stiffness matrix used in a stiffness-based finite element analysis.

3.4.4 Internal stress and strain resultants

Internal stress resultants are composed of axial force, bending moment and shear force at the beam cross-section level. The determination of shear force is decoupled from the axial force and bending moment responses at the section level (Marini & Spacone, 2006). While the fibre beam model calculates the axial force and bending moment as a summation of the axial stresses at each fibre area, the shear force is considered constant through the cross-section and computed at each Gauss point (Martino et al., 2000). The internal stress resultants, \mathbf{p} and the section stiffness matrix, $\mathbf{k}_{\text{section}}$ (the local flexibility matrix, \mathbf{f} is the inverse of $\mathbf{k}_{\text{section}}$ as $\mathbf{f} = \mathbf{k}_{\text{section}}^{-1}$) are determined by the fibre beam formulations with the addition of shear force (Martino et al., 2000; Marini & Spacone, 2006):

$$\mathbf{p} = \begin{bmatrix} N \\ M \\ V \end{bmatrix} = \begin{bmatrix} \sum_{i=1}^{nfibre} \sigma_{fibre} A_{fibre} \\ \sum_{i=1}^{nfibre} \sigma_{fibre} A_{fibre} y_{fibre} \\ V = V(\gamma) \end{bmatrix} \quad (3.29)$$

$$\mathbf{k}_{\text{section}} = \begin{bmatrix} \sum_{i=1}^{nfibre} \left(\frac{d\sigma}{d\varepsilon} \right)_{fibre} A_{fibre} & \sum_{i=1}^{nfibre} \left(\frac{d\sigma}{d\varepsilon} \right)_{fibre} A_{fibre} y_{fibre} & 0 \\ \sum_{i=1}^{nfibre} \left(\frac{d\sigma}{d\varepsilon} \right)_{fibre} A_{fibre} y_{fibre} & \sum_{i=1}^{nfibre} \left(\frac{d\sigma}{d\varepsilon} \right)_{fibre} A_{fibre} y_{fibre}^2 & 0 \\ 0 & 0 & \frac{dV}{d\gamma} \end{bmatrix} \quad (3.30)$$

where $nfibre$ is the number of fibre elements in the cross-section, σ_{fibre} is the axial stress in the fibre, A_{fibre} area of the fibre, y_{fibre} is the distance from the centroid of the cross-section to the centroid of the fibre (Figure 3.8), $\left(\frac{d\sigma}{d\varepsilon} \right)_{fibre}$ is the fibre tangent modulus and $dV/d\gamma$ is the shear tangent modulus. The section stiffness matrix can be represented as a partition of the tangent stiffness contributions of the fibre beam model, $\mathbf{k}_{\text{fibre}}_{(2 \times 2)}$ and the shear behaviour, $dV/d\gamma$ as:

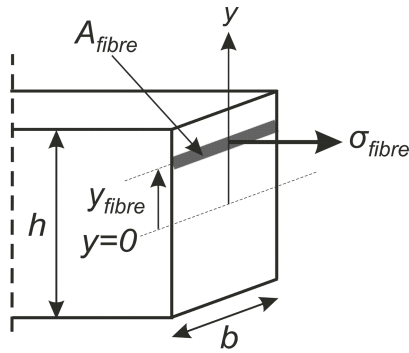


Figure 3.8: Demonstration of a single fibre element at the beam cross-section.

$$\mathbf{k}_{\text{section}} = \left(\frac{\partial \mathbf{p}}{\partial \boldsymbol{\epsilon}} \right) = \begin{bmatrix} \mathbf{k}_{\text{fibre}}_{(2 \times 2)} & \mathbf{0}_{(2 \times 1)} \\ \mathbf{0}_{(1 \times 2)} & dV/dy \end{bmatrix} \quad (3.31)$$

Similarly, the internal stress, \mathbf{p} and strain, $\boldsymbol{\epsilon}$ resultants can be expressed as a partition of the fibre beam and shear behaviour contributions as:

$$\mathbf{p} = \begin{bmatrix} N \\ M \\ V \end{bmatrix} = \begin{bmatrix} \mathbf{p}_{\text{fibre}}_{(2 \times 1)} \\ V \end{bmatrix} \quad \boldsymbol{\epsilon} = \begin{bmatrix} \varepsilon_c \\ \kappa \\ \gamma \end{bmatrix} = \begin{bmatrix} \boldsymbol{\epsilon}_{\text{fibre}}_{(2 \times 1)} \\ \gamma \end{bmatrix} \quad (3.32)$$

where, $\mathbf{p}_{\text{fibre}}_{(2 \times 1)} = [N \quad M]^T$ and $\boldsymbol{\epsilon}_{\text{fibre}}_{(2 \times 1)} = [\varepsilon_c \quad \kappa]^T$.

The axial stress in the fibre needs to be determined according to the material constitutive law for the relationship between the axial strain, ε_i and the axial stress, σ_i , where σ_i is the function of ε_i as $\sigma_i = f(\varepsilon_i)$.

3.4.5 Application of self-weight loads

The self-weight loads of the beam elements are implemented into the flexibility formulations as element loads, which affect the distribution of the internal stress resultants (Taucer et al., 1991; Neuenhofer & Filippou, 1997). The application of self-weight loading is associated with the element loads, \mathbf{p}_0 occurring under uniformly distributed loading applied to a simply supported beam element (Figure 3.9). The self-weight-induced element loads have similar components as the internal stress resultants vector (Equation 3.17):

$$\mathbf{p}_0 = [N_0 \quad M_0 \quad V_0]^T \quad (3.33)$$

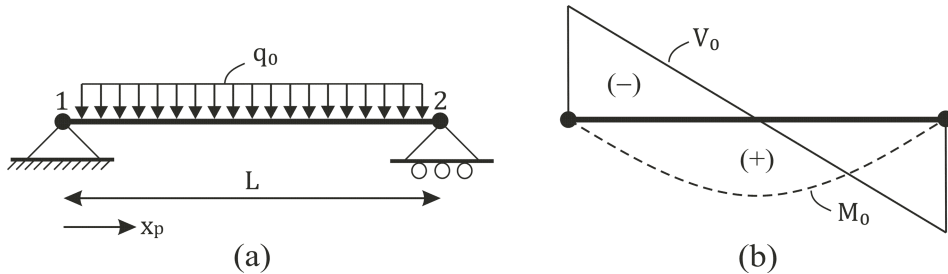


Figure 3.9: A simply supported beam element: (a) under uniformly distributed loading, (b) application of element loads without rigid body modes.

Firstly, the uniformly distributed load applied to the element, q_0 , is calculated using the unit weight of the beam element, γ_m and the cross-sectional dimensions in terms of height, h and width, b of the element as $q_0 = \gamma_m h b$. Then, the element loads are computed for the spandrel $\mathbf{p}_{0,\text{spandrel}}$ and pier, $\mathbf{p}_{0,\text{pier}}$ element orientations as:

$$\mathbf{p}_{0,\text{spandrel}} = q_0 \begin{bmatrix} 0 \\ 1/2(Lx_p - x_p^2) \\ (-L/2 + x_p) \end{bmatrix} \quad \mathbf{p}_{0,\text{pier}} = q_0 \begin{bmatrix} (x_p - L) \\ 0 \\ 0 \end{bmatrix} \quad (3.34)$$

where x_p refers to the position of the Gauss point along the beam length, L , which is defined in the range of $[0, L]$.

The element loads are incorporated in the flexibility formulations at the beginning of the analysis, where only the self-weight loads are applied to the system. To achieve this, the internal stress resultants vector needs to be initialised with the application of element loads. The element loads are determined for the case of a simply supported beam in the absence of rigid body modes in the element level (Figure 3.9b). However, while transferring the internal beam forces to the global equilibrium level, the force reactions at each end of the spandrel/pier must be explicitly included in the global internal nodal force vector (Taucher et al., 1991). Thus, in addition to the nodal internal beam forces calculated in Equation (3.22), the vertical

equilibrium configuration forces (in $+Y$ direction) exerted on the beam element, \mathbf{F}_{eq} is calculated as:

$$\mathbf{F}_{\text{eq,spandrel}} = \mathbf{R}^{-1} [0 \quad q_0 L/2 \quad 0 \quad 0 \quad q_0 L/2 \quad 0]^T \quad (3.35)$$

$$\mathbf{F}_{\text{eq,pier}} = \mathbf{R}^{-1} [q_0 L/2 \quad 0 \quad 0 \quad q_0 L/2 \quad 0 \quad 0]^T \quad (3.36)$$

where, $\mathbf{F}_{\text{eq,spandrel}}$ and $\mathbf{F}_{\text{eq,pier}}$ refer to the spandrel and pier orientations of the beam elements.

The rotation matrix, \mathbf{R} , transforms the rigid body forces computed in the local member coordinates to the global coordinate system.

In the presence of the self-weight loads, in addition to the \mathbf{P}_{beam} vector, the vertical equilibrium configuration forces, \mathbf{F}_{eq} (Equations 3.35 and 3.36), also need to be added into the global internal nodal force vector of the beam elements, $\mathbf{F}_{\text{INT beams}}$. Only for the self-weight analysis $\mathbf{F}_{\text{INT beams}}$ is calculated as:

$$\mathbf{F}_{\text{INT,beams}} = \mathbb{A}[\mathbf{P}_{\text{beam}}] + \mathbb{A}[\mathbf{F}_{\text{eq}}] \quad (3.37)$$

where \mathbb{A} is the assembly operator. In contrast to the stiffness-based finite element formulations, the calculation of external nodal forces is not needed for flexibility-based analysis. Application of self-weight loads to the system is implemented by initialising the internal stress resultants at the beginning of the analysis as element forces determined for simply supported beams.

3.5 Formulation of Stiffness-Based Elements

3.5.1 Quad Elements

Quad element is the key component of a macro-element, which comprises a 4-noded rectangular quad element and continuous interface elements surrounding the edges of the quad element. The quad geometry is determined according to the layout of the façade openings.

Depending on the full rigid offset method (Bracchi et al., 2015), the corners of openings are used to determine the element geometries. This element discretisation approach can be easily applied to the masonry buildings with both regular and irregular façade openings.

The quad element is formulated to translate and rotate as a rigid body while deforming only in shear (Figure 3.10). The interaction of a quad element with adjacent quads or rigid footing elements is governed by the 4-noded edge/line structural interface elements. These deformable interface elements have zero thickness and exert tractions in their normal and tangential directions depending on the relative displacements between two sides of the interface. The normal interface spring stiffness is defined to account for the axial compressibility of the masonry that is defined by the quad element (Caliò et al., 2012).

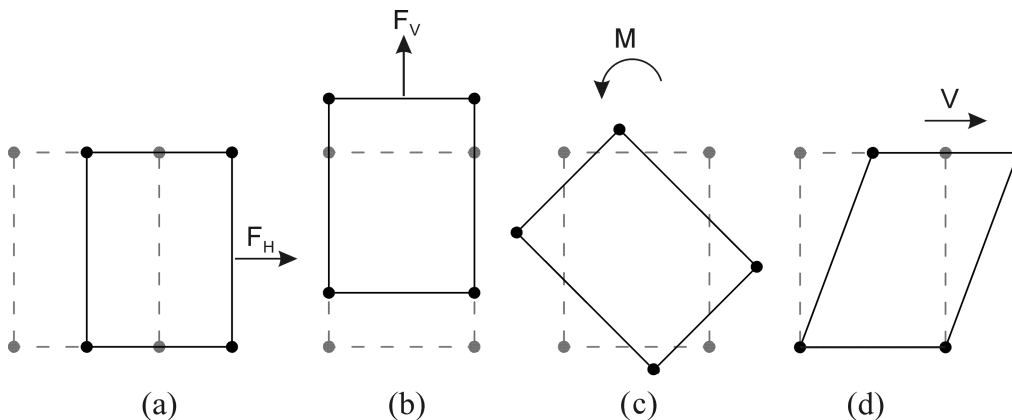


Figure 3.10: The rigid body movements and the deformation mode of a macro-element: (a) axial movement, (b) transverse movement, (c) rotation movement and (d) shear deformation.

3.5.1.1 Kinematics

A quad element (in dimensions of length, L and height, H) with its degrees of freedom (DOF) at the element centroid is demonstrated in Figure 3.11. The quad kinematics is characterised by 4-DOF including horizontal, u_0 and vertical, v_0 displacements, constant shear strain, γ_0 and constant rotation, θ_0 . The quad kinematics presented in the EQFdc model is different than the DOF defined by Caliò et al. (2012).

The displacement vector of a quad element at the centroid, \mathbf{U}_q , is:

$$\mathbf{U}_q = [u_0, v_0, \gamma_0/2, \theta_0]^T \quad (3.38)$$

Consistent with Caliò et al.'s (2012) approach, the quad element does not deform in the axial and transverse directions; the horizontal and vertical strains ε_{xx}^{quad} and ε_{yy}^{quad} are therefore zero.

$$\varepsilon_{xx}^{quad} = \frac{\partial u}{\partial x} = 0; \quad \varepsilon_{yy}^{quad} = \frac{\partial v}{\partial y} = 0 \quad (3.39)$$

where $\frac{\partial u}{\partial x}$ and $\frac{\partial v}{\partial y}$ refer to the partial derivatives of the axial, u and transverse, v displacements.

The quad's motion is characterised by constant shear strain and rotation as:

$$\gamma_0 = \frac{\partial u}{\partial y} + \frac{\partial v}{\partial x}; \quad 2\theta_0 = \frac{\partial v}{\partial x} - \frac{\partial u}{\partial y} \quad (3.40)$$

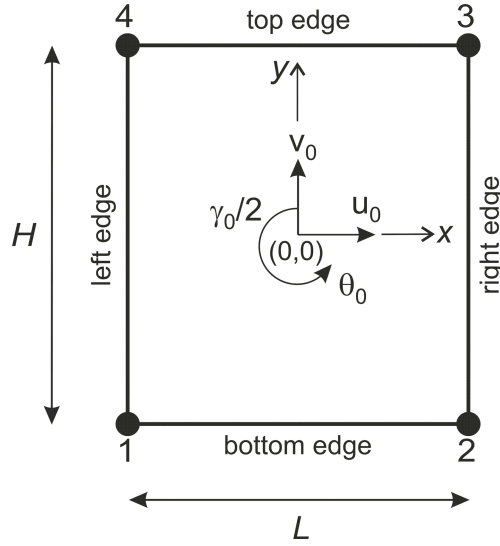


Figure 3.11: Quad element with 4-DOF at the element centroid.

The relationship between the constant shear strain and the 4-DOF of the quad element is:

$$\gamma_0 = \mathbf{B}_q \mathbf{U}_q = [0 \quad 0 \quad 2 \quad 0] \begin{bmatrix} u_0 \\ v_0 \\ \gamma_0/2 \\ \theta_0 \end{bmatrix} \quad (3.41)$$

where \mathbf{B}_q is referred to as the ‘quad kinematic matrix’. The strain and rotation fields in Equation (3.40) define the displacement field of the element in terms of the DOF (Equation 3.42). The axial (u) and transverse (v) displacement fields, determined in the quad local coordinate system (shown by the coordinates x and y in Figure 3.11), are:

$$u = u_0 + \frac{1}{2}(\gamma_0 - 2\theta_0)y; \quad v = v_0 + \frac{1}{2}(\gamma_0 + 2\theta_0)x \quad (3.42)$$

Each quad element interacts with an adjacent quad through interface elements connected to the quads’ edges. To describe relative displacements at the interface, the axial and transverse displacements at each edge of the quad need to be calculated in global coordinates. The displacement vectors at the four edges of the quad, $\mathbf{u} = [u \quad v]^T$, are accordingly derived in the global coordinates, which have the same orientation as local quad coordinates x and y , as indicated in Figure 3.11. The relationship between the displacement vector at the base edge of the quad and the DOF vector is expressed as:

$$\mathbf{u}_B^e = \mathbf{B}_B^e \mathbf{U}_q = \begin{bmatrix} 1 & 0 & -H/2 & H/2 \\ 0 & 1 & x & x \end{bmatrix} \begin{bmatrix} u_0 \\ v_0 \\ \gamma_0/2 \\ \theta_0 \end{bmatrix} \quad (3.43)$$

where \mathbf{u}_B^e is the vector of displacements on the base edge and \mathbf{B}_B^e is the base edge kinematic matrix. Similarly, the displacements on the right, top and left edges (denoted by \mathbf{u}_R^e , \mathbf{u}_T^e and \mathbf{u}_L^e) of the quad are formulated by using the right, top and left edge kinematic matrices (expressed by \mathbf{B}_R^e , \mathbf{B}_T^e and \mathbf{B}_L^e) as given in Equations (3.44) – (3.46).

$$\mathbf{u}_R^e = \mathbf{B}_R^e \mathbf{U}_q = \begin{bmatrix} 1 & 0 & y & -y \\ 0 & 1 & L/2 & L/2 \end{bmatrix} \begin{bmatrix} u_0 \\ v_0 \\ \gamma_0/2 \\ \theta_0 \end{bmatrix} \quad (3.44)$$

$$\mathbf{u}_T^e = \mathbf{B}_T^e \mathbf{U}_q = \begin{bmatrix} 1 & 0 & H/2 & -H/2 \\ 0 & 1 & x & x \end{bmatrix} \begin{bmatrix} u_0 \\ v_0 \\ \gamma_0/2 \\ \theta_0 \end{bmatrix} \quad (3.45)$$

$$\mathbf{u}_L^e = \mathbf{B}_L^e \mathbf{U}_q = \begin{bmatrix} 1 & 0 & y & -y \\ 0 & 1 & -L/2 & -L/2 \end{bmatrix} \begin{bmatrix} u_0 \\ v_0 \\ \gamma_0/2 \\ \theta_0 \end{bmatrix} \quad (3.46)$$

3.5.1.2 Internal forces and stiffness matrix

The internal virtual work of a quad element, $\delta W_{int,quad}$ is formulated as:

$$\delta W_{int,quad} = \int_0^V (\delta \gamma_0)^T \tau dV \quad (3.47)$$

where $\delta \gamma_0$ is the virtual shear strain, τ is the shear stress and V is the element volume.

Determination of shear stress depends on the constitutive model used for the quad element (Sections 5.4.1 and 6.3.1). The internal force vector, $\mathbf{f}_{int,quad}$ and the stiffness matrix, \mathbf{K}_{quad} of the quad element are derived in (4×1) and (4×4) forms, respectively as:

$$\mathbf{f}_{int,quad} = \int_0^V \mathbf{B}_q^T \left(\frac{d\tau}{d\gamma_0} \right) \mathbf{B}_q \mathbf{U}_q dV \quad (3.48)$$

$$\mathbf{K}_{quad} = \mathbf{B}_q^T \left(\frac{d\tau}{d\gamma_0} \right) \mathbf{B}_q t_q L H \quad (3.49)$$

where $\left(\frac{d\tau}{d\gamma_0} \right)$ is the quad tangent modulus (depends on the constitutive model used for the quad),

t_q is the quad thickness and dV is an infinitesimal volume element.

3.5.1.3 External forces

The external virtual work associated with a quad element, $\delta W_{ext,quad}$ is,

$$\delta W_{ext,quad} = - \int \delta v \gamma_q dV \quad (3.50)$$

where δv is the virtual vertical displacement, γ_q is the unit weight of the quad. The self-weight vector of a quad element, $\mathbf{f}_{ext,quad}$ can be calculated directly as:

$$\mathbf{f}_{ext,quad} = -[0 \quad H \ L \ t_q \ \gamma_q \quad 0 \quad 0]^T \quad (3.51)$$

3.5.2 Footing Elements

Footing elements (Figure 3.12) are modelled between the quad elements below the ground level and the soil-foundation interface elements (Figure 3.3c).

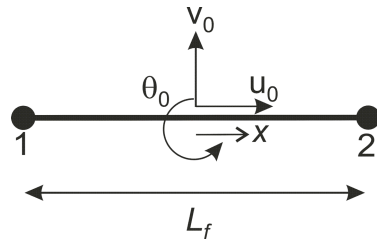


Figure 3.12: Footing element with 3-DOF at the element centroid.

3.5.2.1 Kinematics

The footing element is modelled as a rigid bar element composed of 3-DOF at the element centroid (Figure 3.12). The rigid footing element ensures that the displacement fields of the footing elements are consistent with the edge displacements of the quad elements just above.

The footing element DOF vector, \mathbf{U}_f , is formulated in (3×1) form as:

$$\mathbf{U}_f = [u_0 \quad v_0 \quad \theta_0]^T \quad (3.52)$$

Thus, the local displacement vector along the footing x -axis, $\mathbf{u}_f = [u \quad v]^T$ is determined as:

$$\mathbf{u}_f = \mathbf{B}_f \mathbf{U}_f = \begin{bmatrix} 1 & 0 & 0 \\ 0 & 1 & x \end{bmatrix} \begin{bmatrix} u_0 \\ v_0 \\ \theta_0 \end{bmatrix} \quad (3.53)$$

where \mathbf{B}_f is the footing kinematic matrix, x is any point along x -axis ($x \in [-L_f/2, L_f/2]$) and L_f is the length of the footing element.

3.5.2.2 Internal forces and stiffness matrix

In the rigid footing (bar) elements, deformation is prevented. The internal virtual work of a rigid footing element is therefore zero.

3.5.2.3 External forces

The self-weight vector of the footing element, $\mathbf{f}_{\text{ext,footing}}$ is given as:

$$\mathbf{f}_{\text{ext,footing}} = -[0, h_f L_f t_f \gamma_f, 0]^T \quad (3.54)$$

where h_f , L_f , t_f and γ_f are the height, length, width and unit weight of the footing, respectively.

3.5.3 Structural Interface Elements

Structural interface elements are classified according to the type of elements they connect. They are referred to as quad-quad, quad-beam, quad-footing and footing-footing interface elements in the EQFdc model.

3.5.3.1 Kinematics

Quad-quad interface elements

The interface elements between the adjacent quad elements are formulated according to the orientation of the interface in the vertical or horizontal directions (Figures 3.13 and 3.14). The interface local coordinate system is indicated with relative displacements in shear, u_r and normal, v_r directions.

The relative displacements in the interface elements, $\mathbf{u}_r = [u_r \ v_r]^T$ are determined using the edge kinematic matrices and the element displacement vectors of the adjacent quad elements

for vertical (Equation 3.55) and horizontal interface orientations (Equation 3.56).

$$\mathbf{u}_r = \mathbf{T} [\mathbf{B}_L^{\text{right}} \quad -\mathbf{B}_R^{\text{left}}] \begin{bmatrix} \mathbf{U}^{\text{right}} \\ \mathbf{U}^{\text{left}} \end{bmatrix} \quad (3.55)$$

$$\mathbf{u}_r = \mathbf{T} [\mathbf{B}_B^{\text{upper}} \quad -\mathbf{B}_T^{\text{lower}}] \begin{bmatrix} \mathbf{U}^{\text{upper}} \\ \mathbf{U}^{\text{lower}} \end{bmatrix} \quad (3.56)$$

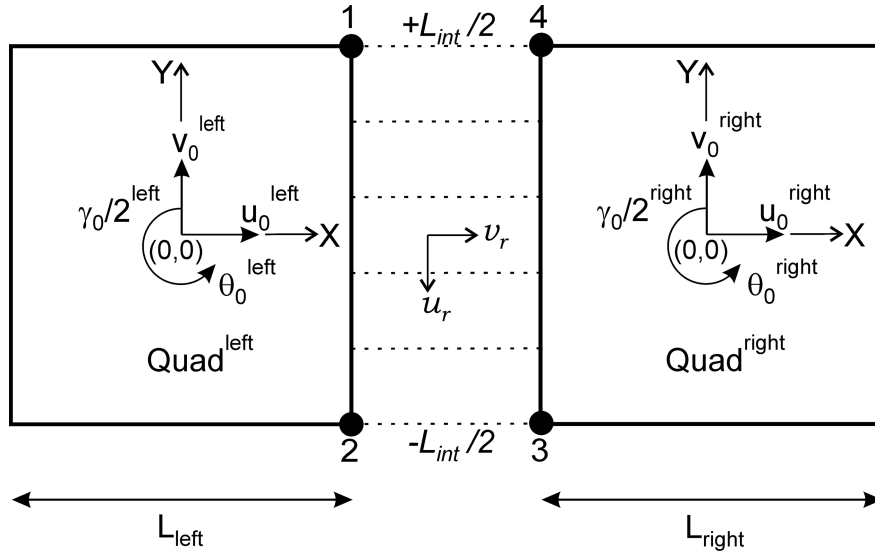


Figure 3.13: Quad-quad interface element in the vertical orientation.

where $\mathbf{B}_L^{\text{right}}$, $\mathbf{B}_R^{\text{left}}$, $\mathbf{B}_B^{\text{upper}}$ and $\mathbf{B}_T^{\text{lower}}$ are the edge kinematic matrices (i.e. the superscript and subscript refer to the quad element position and its corresponding edge, respectively) in (2×4) form defined in Equations (3.43) – (3.46). $\mathbf{U}^{\text{right}}$ is the element displacement vector for the right quad element written in (4×1) form. Similarly, \mathbf{U}^{left} , $\mathbf{U}^{\text{upper}}$ and $\mathbf{U}^{\text{lower}}$ are the element displacement vectors of the left, upper and lower quads, respectively. Additionally, \mathbf{T} is a transformation matrix in (2×2) form used to transform the relative displacements calculated in the global coordinate system to the local coordinates of the interfaces. The relative displacement calculation can be written in a compact form by generalising the interface edge kinematic matrix as \mathbf{B}_{int} and the interface element displacement vector as \mathbf{U}_{int} :

$$\mathbf{u}_r = \mathbf{T}\mathbf{B}_{int}\mathbf{U}_{int} \quad (3.57)$$

where \mathbf{B}_{int} is in (2×8) and \mathbf{U}_{int} is in (8×1) form for the quad-quad interface elements.

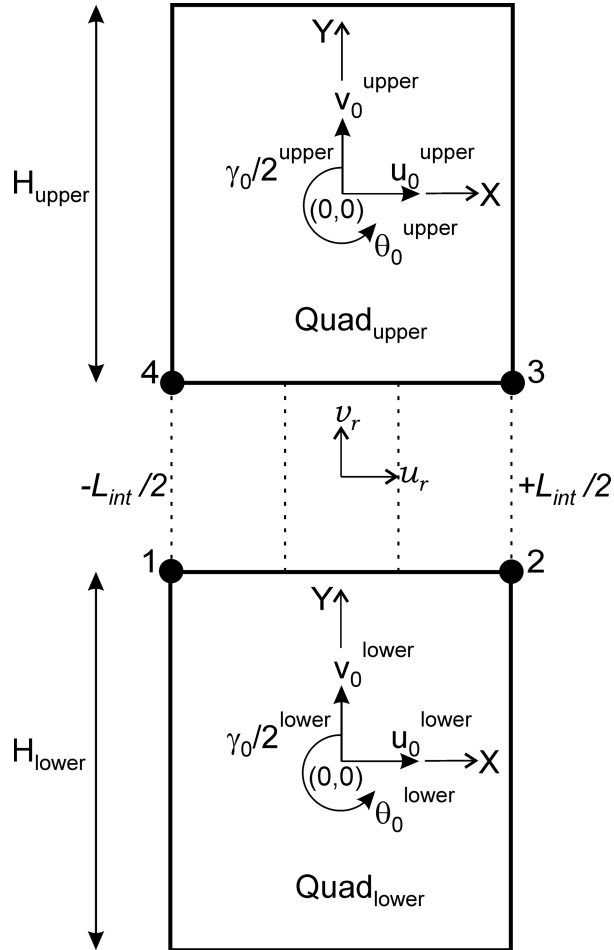


Figure 3.14: Quad-quad interface element in horizontal orientation.

Quad-beam interface elements

In the quad-beam interfaces, the beam edges are connected rigidly to the quad's edges (Figure 3.15). The kinematics of quad-beam interfaces are defined with 7-DOF, in which 4-DOF is from the quad element and 3-DOF is from the beam element. Notably, the normal stiffness of the quad-beam interface element only depends on the contribution of the quad element since the axial compliance of the beam is incorporated in the beam element formulation. The beam's start and end node displacements are expressed with the vectors $\mathbf{U}_{beam,i}$ and $\mathbf{U}_{beam,i+1}$ in

(3×1) forms separately. Accordingly, the global u_B and v_B displacements at any point along with the beam height, $-L_{int}/2 \leq h \leq L_{int}/2$, are calculated at $x = 0$ for the beam's left edge and at $x = L$ for the beam's right edge as given as follows:

$$\begin{bmatrix} u_B^{\text{left}} \\ v_B^{\text{left}} \end{bmatrix} = \mathbf{B}_h \mathbf{U}_{\text{beam},i} = \mathbf{B}_h \begin{bmatrix} u_{B,i} \\ v_{B,i} \\ \theta_{B,i} \end{bmatrix} \quad (3.58)$$

$$\begin{bmatrix} u_B^{\text{right}} \\ v_B^{\text{right}} \end{bmatrix} = \mathbf{B}_h \mathbf{U}_{\text{beam},i+1} = \mathbf{B}_h \begin{bmatrix} u_{B,i+1} \\ v_{B,i+1} \\ \theta_{B,i+1} \end{bmatrix} \quad (3.59)$$

where the edge kinematic matrix along the beam height, \mathbf{B}_h , is derived in the global coordinates of the spandrel (Equation 3.60) and pier (Equation 3.61) elements as:

$$\mathbf{B}_h = \begin{bmatrix} 1 & 0 & -h \\ 0 & 1 & 0 \end{bmatrix} \quad (3.60)$$

$$\mathbf{B}_h = \begin{bmatrix} 1 & 0 & 0 \\ 0 & 1 & -h \end{bmatrix} \quad (3.61)$$

The relative displacements at the beam left edge interface, \mathbf{u}_r , are computed as:

$$\mathbf{u}_r = \mathbf{T}(\mathbf{B}_{\text{quad-beam}}^{\text{left}} \mathbf{U}_{\text{quad-beam}}^{\text{left}}) = \mathbf{T}\left(\left[\mathbf{B}_h \quad -\mathbf{B}_{\text{quad},iR}\right] \begin{bmatrix} \mathbf{U}_{\text{beam},i} \\ \mathbf{U}_{\text{quad},i} \end{bmatrix}\right) \quad (3.62)$$

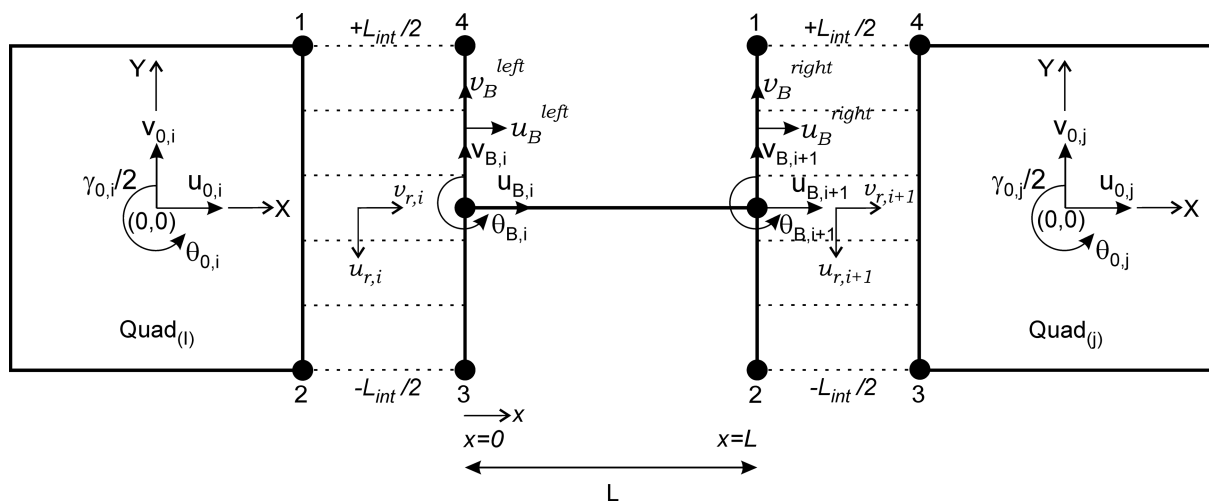


Figure 3.15: The quad-beam interface connection.

where $\mathbf{B}_{\text{quad-beam}}^{\text{left}}$ is the combined (2×7) form of edge kinematic matrices for the beam left edge interface. $\mathbf{B}_{\text{quad-beam}}^{\text{left}}$ comprises the edge kinematic matrix, \mathbf{B}_h , along the beam height and the right edge kinematic matrix of the quad element, $\mathbf{B}_{\text{quad},iR}$, which is connected to the beam's left edge. The edge kinematic matrices of \mathbf{B}_h and $-\mathbf{B}_{\text{quad},iR}$ are the sub-matrices of $\mathbf{B}_{\text{quad-beam}}^{\text{left}}$ and they are formulated in (2×3) and (2×4) forms, respectively. Similarly, $\mathbf{U}_{\text{quad-beam}}^{\text{left}}$ is the combination of DOF vectors which is formulated in (7×1) form, including the DOF vector of the beam element at the start node, $\mathbf{U}_{\text{beam},i}$ and the element displacement vector of the Quad_i, $\mathbf{U}_{\text{quad},i}$. Additionally, \mathbf{T} is a transformation matrix derived in (2×2) form. Since both quad and beam edge kinematic matrices are formulated in global coordinates, \mathbf{T} matrix is needed to transform the relative displacements computed in the structure's global coordinates to the interface elements' local coordinates. Similarly, the relative displacements at the beam right edge interface are computed as:

$$\mathbf{u}_r = \mathbf{T} \left(\mathbf{B}_{\text{quad-beam}}^{\text{right}} \mathbf{U}_{\text{quad-beam}}^{\text{right}} \right) = \mathbf{T} \left(\begin{bmatrix} \mathbf{B}_{\text{quad},jL} & -\mathbf{B}_h \end{bmatrix} \begin{bmatrix} \mathbf{U}_{\text{quad},j} \\ \mathbf{U}_{\text{beam},i+1} \end{bmatrix} \right) \quad (3.63)$$

In this case, $\mathbf{B}_{\text{quad-beam}}^{\text{right}}$ is the combined (2×7) form of the edge kinematic matrices derived at the left edge of the quad ($\mathbf{B}_{\text{quad},jL}$) and at the right edge of the beam (\mathbf{B}_h). Similarly, $\mathbf{U}_{\text{quad-beam}}^{\text{right}}$ represents the compact (7×1) form of the DOF vectors belonging to the Quad_j, $\mathbf{U}_{\text{quad},j}$ and the beam's end node, $\mathbf{U}_{\text{beam},i+1}$.

Quad-footing interface elements

The quad-footing interface elements connect the base edge of the quads and the centroidal axis of the footing elements (Figure 3.16). In this approach, a quad is employed to represent the underground part of the masonry wall with a height of h_{wg} (Figure 3.16a). The height of the quad is determined as $h_{qg} = h_{wg} + h_f/2$, which extends up to the centroidal axis of the footing

element (Figure 3.16b). Here, h_f represents the height of the rectangular footing cross-section. Thus, the quad-footing interface connects the underground section of the masonry wall to the rigid footing element (which represents the wide strip with a width of t_f and length of L_f) interacting with the soil underneath. The relative displacements in the quad-footing interface are derived in Equation (3.64). In this case, \mathbf{B}_{qf} is the edge kinematic matrix and \mathbf{U}_{qf} is the element displacement vector of the quad-footing interface.

$$\mathbf{u}_r = \mathbf{B}_{qf} \mathbf{U}_{qf} = [\mathbf{B}_B^{\text{upper}} \quad -\mathbf{B}_f] \begin{bmatrix} \mathbf{U}_B^{\text{upper}} \\ \mathbf{U}_f \end{bmatrix} \quad (3.64)$$

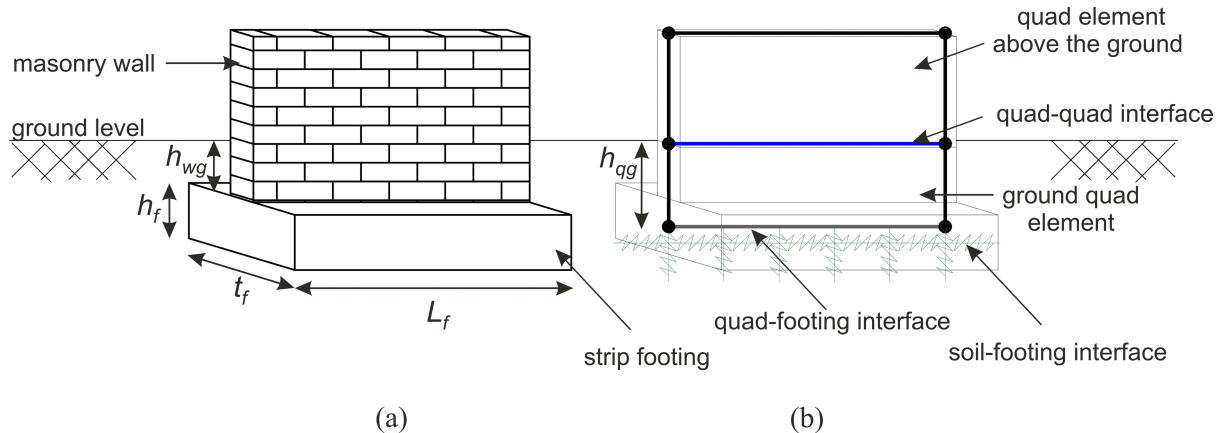


Figure 3.16: Modelling of the masonry section underground: (a) footing detail, (b) quad-footing interface detail.

Footing-footing interface elements

Between the nodes of the footing elements (e.g. node denoted as $i + 1$ and $i + 2$), 2-noded axial springs are used as compliant elements to allow the deformations between the adjacent rigid footing elements (Figure 3.17).

The relative displacements between footing elements are calculated using the kinematic matrix, \mathbf{B}_{ff} and the element displacement vector, \mathbf{U}_{ff} of the footing-footing interface elements, which are derived in (2×6) and (6×1) forms as:

$$\mathbf{u}_r = \mathbf{B}_{ff} \mathbf{U}_{ff} = \begin{bmatrix} 1 & 0 & 0 & -1 & 0 & 0 \\ 0 & 0 & 0 & 0 & 0 & 0 \end{bmatrix} \begin{bmatrix} \mathbf{U}_f^{\text{right}} \\ \mathbf{U}_f^{\text{left}} \end{bmatrix} \quad (3.65)$$

where $\mathbf{U}_f^{\text{right}}$ and $\mathbf{U}_f^{\text{left}}$ refer to the element displacement vectors of the adjacent footings.

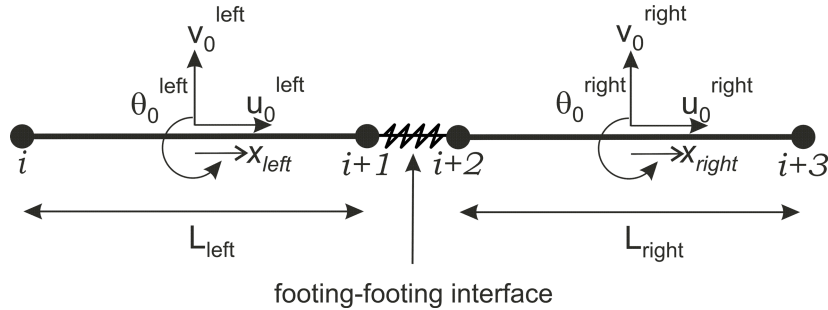


Figure 3.17: Footing-footing interface.

3.5.3.2 Internal forces and stiffness matrix

The normal stiffness of each interface element represents the elastic stiffness of the masonry portion corresponding to the influenced area of the quad element (Caliò et al., 2012; Minga, 2017). Figure 3.18 shows the definition of interface influence areas for the vertical (Figure 3.18a) and horizontal (Figure 3.18b) orientation of the quad-quad interfaces. The shear, $K_{s,i}$ and normal, $K_{n,i}$ stiffness contributions of a corresponding quad in an interface element are computed as:

$$K_{s,i} = 10^6 K_{n,i} \quad K_{n,i} = \frac{E_i}{L_i/2} \quad (3.66)$$

where the interface influence length that considers the half dimension of the corresponding quad element, such as $L_i/2$ and $H_i/2$, for the vertical and horizontal interface elements associated with Quad_i. For the adjacent Quad_i and Quad_j elements (Young's modulus are E_i and E_j whereas the interface influence lengths are L_i and L_j respectively), the normal stiffness of the interface element, $K_{n,int}$ computed as:

$$K_{n,int} = \frac{K_{n,i} K_{n,j}}{K_{n,i} + K_{n,j}} = \frac{E_i E_j}{E_j L_i + E_i L_j} \quad (3.67)$$

where $K_{n,i}$ and $K_{n,j}$ refer to the normal stiffness contributions of Quad_i and Quad_j, respectively.

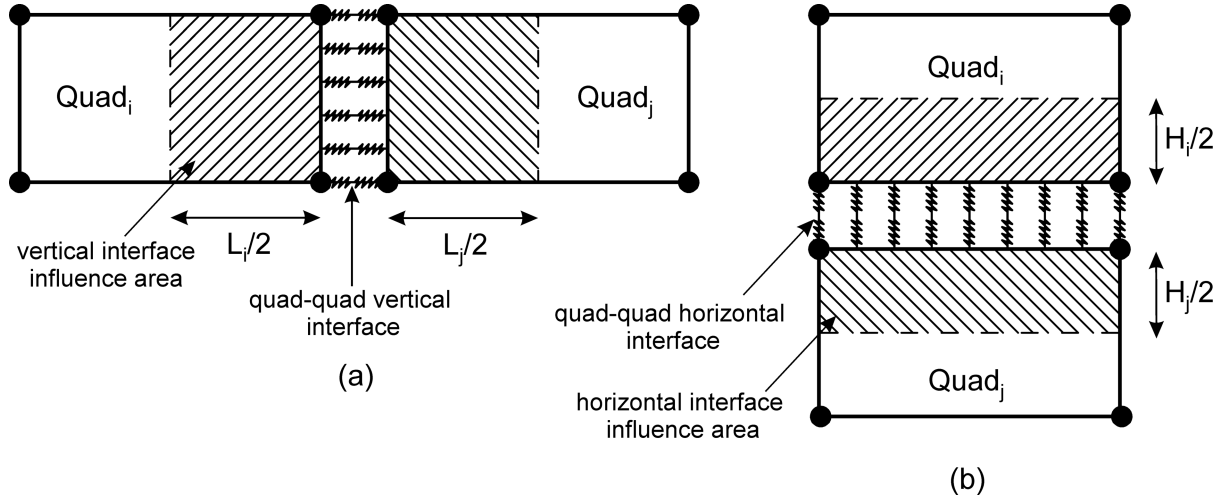


Figure 3.18: Quad-quad interface influence area: (a) vertical orientation, (b) horizontal orientation.

For the quad-footing interface elements (Figure 3.19), $K_{n,int}$ only depends on the ground quad element's stiffness contribution. For the footing-footing interface, the axial stiffness contributions of the footing elements at the right, K_r and the left, K_l sides of the nodes are employed to determine the constitutive matrix of the axial spring, $\mathbf{D}_{\text{Spring}}$ as follows:

$$\mathbf{D}_{\text{Spring}} = \begin{bmatrix} K_r K_l / (K_r + K_l) & 0 \\ 0 & 0 \end{bmatrix} \quad (3.68)$$

$$K_r = \frac{E_r A_f}{L_r/2} \quad K_l = \frac{E_l A_f}{L_l/2} \quad (3.69)$$

where E_r and E_l are the Young's modulus, L_r and L_l are the length and A_f is the cross-sectional area of the footing elements at the right and left sides of the shared footing node.

The internal virtual work of an interface element is related to the relative displacements, \mathbf{u}_r and the tractions, \mathbf{p} . The traction vector, $\mathbf{p} = [t \quad p]^T$ is composed of shear, t and normal p

tractions computed in the local coordinates of the interface element. The internal virtual work of any interface element, $\delta W_{int,interface}$ is determined by,

$$\delta W_{int,interface} = \int_{-L_{int}/2}^{L_{int}/2} (\delta \mathbf{u}_r)^T \mathbf{p} t_{int} dX \quad (3.70)$$

where $\delta \mathbf{u}_r$ is the virtual relative displacements, L_{int} is the interface length and t_{int} is the interface thickness. For the horizontal quad-quad interface, L_{int} is the quad length and the integration is performed over the global X axis. In contrast, for the vertical quad-quad interface, L_{int} is the quad height and the integration is performed over the global Y axis. The internal force vector, $\mathbf{f}_{int,interface}$ and the element stiffness matrix, $\mathbf{K}_{int,interface}$ of the interface elements are represented in terms of the interface tangent modulus, $\left(\frac{d\mathbf{p}}{d\mathbf{u}_r}\right)$ (depends on the constitutive model used for the interface element) as follows:

$$\mathbf{f}_{int,interface} = \int_{-L_{int}/2}^{L_{int}/2} (\mathbf{T}\mathbf{B}_{int})^T \left(\frac{d\mathbf{p}}{d\mathbf{u}_r}\right) (\mathbf{T}\mathbf{B}_{int}) \mathbf{U}_{int} t_{int} dX \quad (3.71)$$

$$\mathbf{K}_{int,interface} = \int_{-L_{int}/2}^{L_{int}/2} (\mathbf{T}\mathbf{B}_{int})^T \left(\frac{d\mathbf{p}}{d\mathbf{u}_r}\right) (\mathbf{T}\mathbf{B}_{int}) t_{int} dX \quad (3.72)$$

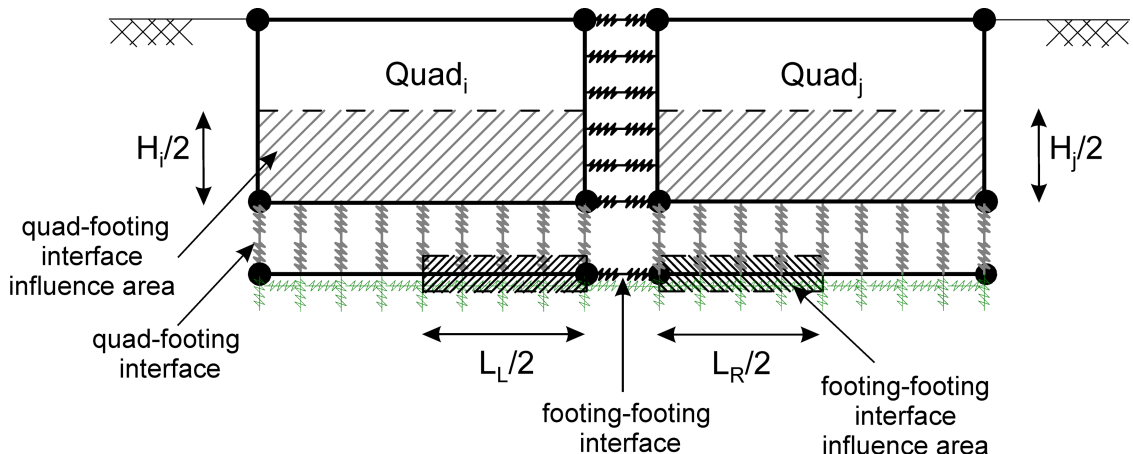


Figure 3.19: Quad-footing and footing-footing interface influence areas.

where t_{int} is the quad thickness (t_q) for the quad-quad and quad-beam interface elements and it represents the footing width (t_f) for the quad-footing interfaces. Note that when calculating footing-footing interfaces, the thickness parameter, t_{int} , needs to be removed from the internal force vector and the stiffness matrix equations.

Here, according to the type of interface elements, the specific edge kinematic matrices need to be used in place of \mathbf{B}_{int} and the specific element displacement vectors in place of \mathbf{U}_{int} . Similarly, the element constitutive matrix, $\mathbf{D}_{int} = [K_{s,int} \ 0 ; 0 \ K_{n,int}]$ (i.e. $K_{s,int}$ is the shear stiffness and $K_{n,int}$ is the normal stiffness of the interface element) needs to be chosen according to the type of interface elements. The relative displacements calculated in the global coordinate system need to be transformed to the local coordinates of the interface element by using the transformation matrix, \mathbf{T} in (2×2) form. When the quad-beam interface is orientated vertically, the integrations are performed over the global Y axis as dY . Likewise, dX is used for the global X axis for the horizontal interface orientation.

3.6 Determination of Strain Distributions

Calculation of major principal tensile strains is required to determine the damage class in a tunnel-soil-structure interaction problem.

3.6.1 Macro-elements

To find the strains experienced by the macro-element (i.e. combination of a quad and surrounding interfaces) and consequently, the masonry structure it represents, it is necessary to develop a procedure that accounts for the combination of shear strains inside the quad and the transverse deformations of the interface. The procedure involves setting up an internal grid in axial and transverse directions within the macro-element (Figure 3.20). The quad element experiences uniform shear strain (γ_0) and zero plane strains in axial and transverse directions.

The interfaces idealise the axial and transverse deformability of the masonry. Thus, the deformations that the interfaces experience can be attributed to the grids inside the macro-element (Figure 3.20). Since the relative shear displacements in the interface elements are expected to be negligible due to the high value of interface shear stiffness, only the relative normal displacements are considered.

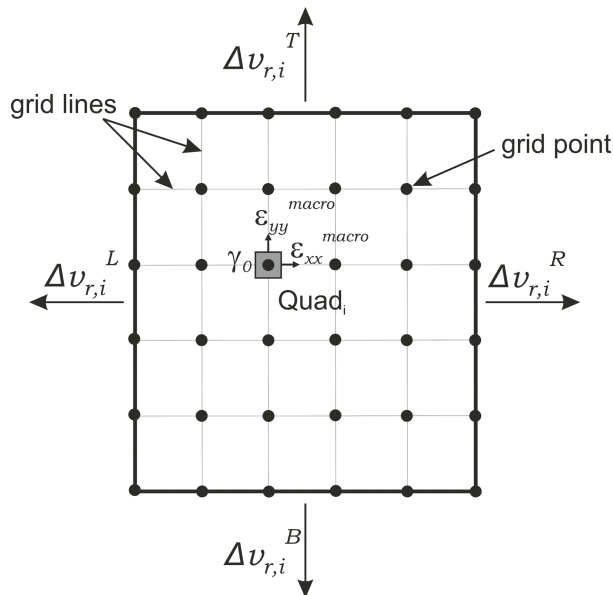


Figure 3.20: A macro-element showing the internal grids and the relative normal displacements induced by Quad_i at the quad edges.

The total relative displacements at the interfaces arise due to the deformation of adjacent quads. To find the plane strains at the grid points of a macro-element in axial, ε_{xx}^{macro} and transverse, ε_{yy}^{macro} directions, it is necessary to partition off the total interface relative displacements into components that belong to each macro-element. This is achieved by noting that each interface spring is composed of two springs arranged in series. K_B , K_T , K_R and K_L are the total normal stiffness modulus at the bottom, top, right and left edge interfaces surrounding the quad, Quad_i. Accordingly, $K_{B,i}$, $K_{T,i}$, $K_{R,i}$ and $K_{L,i}$ are the normal stiffness modulus contributions of the quad, Quad_i to the total normal stiffness modulus. The relative normal displacements induced by Quad_i at the bottom, top, right and left ($\Delta v_{r,i}^B$, $\Delta v_{r,i}^T$, $\Delta v_{r,i}^R$ and $\Delta v_{r,i}^L$ respectively, where

superscript refers to the quad edge) interfaces are computed at each grid along the edges:

$$\Delta v_{r,i}^B = \frac{K_B}{K_{B,i}} v_r^B, \quad \Delta v_{r,i}^T = \frac{K_T}{K_{T,i}} v_r^T, \quad \Delta v_{r,i}^R = \frac{K_R}{K_{R,i}} v_r^R, \quad \Delta v_{r,i}^L = \frac{K_L}{K_{L,i}} v_r^L \quad (3.73)$$

Then, ε_{xx}^{macro} and ε_{yy}^{macro} are computed at each grid point inside the macro-element:

$$\varepsilon_{xx}^{macro} = \frac{\Delta v_{r,i}^R + \Delta v_{r,i}^L}{L} \quad \varepsilon_{yy}^{macro} = \frac{\Delta v_{r,i}^T + \Delta v_{r,i}^B}{H} \quad (3.74)$$

where L is the length and H is the height of the quad. Finally, the major principal tensile strain, ε_1 is computed at each grid point as:

$$\varepsilon_1 = \frac{\varepsilon_{xx}^{macro} + \varepsilon_{yy}^{macro}}{2} + \sqrt{\frac{(\varepsilon_{xx}^{macro} - \varepsilon_{yy}^{macro})^2 + \gamma_0^2}{4}} \quad (3.75)$$

3.6.2 Beam elements

In the flexibility-based beam element formulations, the axial strain is computed and stored in a database, $\boldsymbol{\varepsilon}_{\text{fibre}}^{\text{database}}$ for each corresponding beam (*ibeam*), Gauss point (*igauss*) and fibre element (*ifibre*). Thus, the axial strain in the x -axis of the cross-section, ε_{xx} , is extracted from the axial strain database as $\varepsilon_{xx} = \boldsymbol{\varepsilon}_{\text{fibre}}^{\text{database}}(\text{ibeam}, \text{igauss}, \text{ifibre})$. However, the transverse strain in y -axis is considered zero, $\varepsilon_{yy} = 0$. At the end of the flexibility analysis, the shear strains are extracted from the internal strain resultants vector as $\boldsymbol{\gamma} = \boldsymbol{\varepsilon}(3)$. The shear strain is formulated as constant across the beam cross-section as mentioned in the flexibility formulations. However, while post processing the analysis results for the calculation of the major principal tensile strain, a parabolic distribution of the shear strain is assumed for a linear elastic beam model. In contrast, the constant shear strain approach is maintained for the nonlinear beam model. The distribution of major principal tensile strains in a beam element is computed at each fibre element across the cross-section and along each Gauss point.

3.7 Conclusion

In this chapter, the formulation of a novel EQFdc model is explained. The modelling approach combines the advantageous features of both EQF (i.e. with rigid connectors used widely in the earthquake engineering field) and macro-element models. This is achieved by representing the frame behaviour through spandrels and piers according to the EQF modelling approach but by replacing the rigid connectors with the deformable macro-elements to eliminate the overestimation of building stiffness. Using macro-elements in the EQFdc modelling approach also solves the uncertainties specified in the idealisations of element geometries in the original EQF models because the macro-element idealisation of the masonry buildings is quite straightforward and can be applied to both façades with regular and irregular openings easily. The EQFdc model also provides a practical method to represent the building and foundation interaction by modelling the embedded portion of the façade below the ground level with the quad elements and employing footing elements underneath to allow the connection with soil-foundation interface elements.

Flexibility-based beam element formulations are used to model the spandrels and the piers in the EQFdc model. Flexibility-based formulations are chosen since they can easily be incorporated with the 1D nonlinear constitutive material models (Chapter 6). The macro-elements are modelled with the stiffness-based formulations, but the kinematics formulation allows for practically representing the quad shear behaviour and translational deformations in the interface elements. Conveniently, these can also be represented with the same 1D nonlinear constitutive material models used for beams.

The EQFdc model enables the determination of major principal tensile strains to estimate the damage class of masonry buildings affected by tunnelling-induced displacements based on the standard building damage classification system that is widely used in the tunnelling industry.

Chapter 4

EQFdc Analysis: Solution Procedure

4.1 Introduction

A general solution procedure employed for both linear and nonlinear analyses in the EQFdc model is explained in this chapter. The EQFdc analysis comprises three main iteration procedures conducted at global, element and Gauss point levels for both linear and nonlinear analysis. The global level is defined for the whole structure, including the quad, the beam and the interface elements. However, the element and cross-section levels are only required for the beams, which are modelled according to the flexibility formulations.

4.2 Global Level Iteration

The general solution procedure used for the EQFdc analysis in the global equilibrium level comprising the whole elements is explained in this section. Figure 4.1 shows the summary of the EQFdc analysis solution procedure, which starts iterating to satisfy the equilibrium at the global level and then updates the global internal forces in each element. The global internal forces are computed based on the finite element formulations adopted for the specified element (i.e. either according to stiffness-based or flexibility-based formulations). The aim is to find an equilibrium between the external global forces applied to the system, \mathbf{F}_{EXT} and the internal global forces \mathbf{F}_{INT} computed for each element depending on the specified constitutive models.

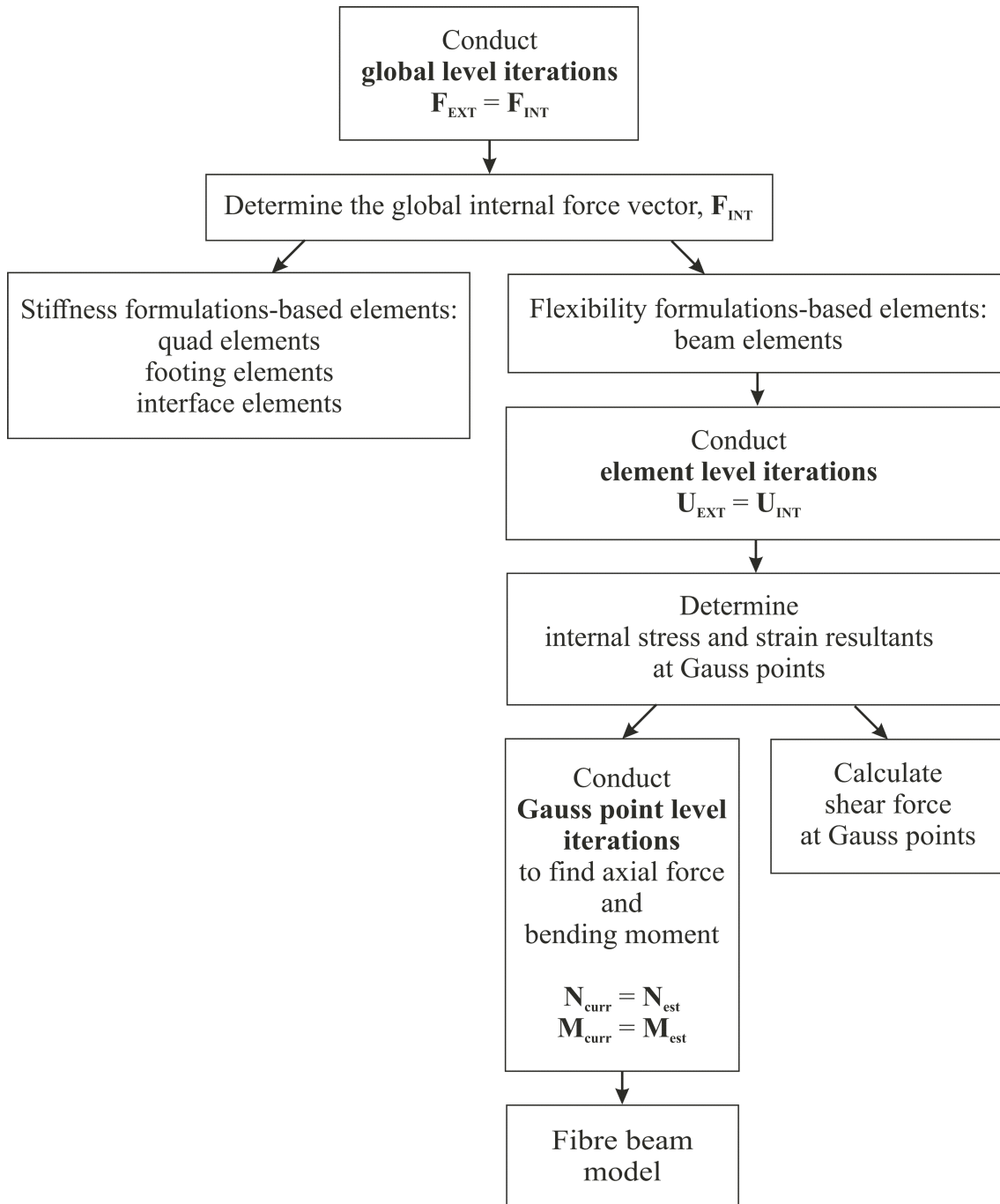


Figure 4.1: The general solution procedure for the EQFdc analysis.

External loads are applied to the model in steps. At each global iteration, the equilibrium between the external and internal global forces are checked to satisfy:

$$\mathbf{G}(\mathbf{U}_{ite}) = \mathbf{F}_{EXT} - \mathbf{F}_{INT}(\mathbf{U}_{ite}) \quad (4.1)$$

where \mathbf{G} is the out-of-balance force vector at the global (whole structure) level and \mathbf{U}_{ite} is the

global nodal displacement vector at the specified global iteration number ('ite'). The solution to the global force equilibrium is sought to find the corresponding \mathbf{U}_{ite} that satisfies $\mathbf{G} = 0$. To solve Equation (4.1), $\mathbf{G}(\mathbf{U})$ is linearised at $\mathbf{U} = \mathbf{U}_{\text{ite}}$ as:

$$\mathbf{G}(\mathbf{U}) \approx \mathbf{G}(\mathbf{U}_{\text{ite}}) + \frac{\partial \mathbf{G}}{\partial \mathbf{U}} \Delta \mathbf{U} \quad (4.2)$$

where $\Delta \mathbf{U} = \mathbf{U} - \mathbf{U}_{\text{ite}}$ is the incremental global nodal displacements and $\frac{\partial \mathbf{G}}{\partial \mathbf{U}}$ is the global tangent stiffness matrix.

The Modified Newton Raphson iteration scheme is used to solve Equation (4.2) for the specified global nodal displacements vector of \mathbf{U}_{ite} . First, the internal global force vector, $\mathbf{F}_{\text{INT}}(\mathbf{U}_{\text{ite}})$, is calculated for all elements in the model and then the global force out-of-balance vector is determined for the specified global iteration as $\mathbf{G}(\mathbf{U}_{\text{ite}})$. Here, it is important to note that the calculation of the internal global force vector for the beam elements require complex iterative procedures for the flexibility analysis that described in the next sections. If $\|\mathbf{G}(\mathbf{U}_{\text{ite}})\| < tol$, where tol is the global tolerance value chosen as 10 N (or 10 Nm), then the result of the current iteration is selected as $\mathbf{U} = \mathbf{U}_{\text{ite}}$. Otherwise, the incremental global nodal displacements, $\Delta \mathbf{U}$, are computed by solving,

$$0 = \mathbf{G}(\mathbf{U}_{\text{ite}}) + \frac{\partial \mathbf{G}}{\partial \mathbf{U}} \Delta \mathbf{U} \quad (4.3)$$

The nodal displacement vector is then updated for the next iteration as follows:

$$\mathbf{U}_{\text{ite+1}} = \mathbf{U}_{\text{ite}} + \Delta \mathbf{U} \quad (4.4)$$

The process continues to iterate until $\|\mathbf{G}(\mathbf{U}_{\text{ite+1}})\| < tol$.

The global level iterations are performed separately for the self-weight and the greenfield displacement loadings. For the EQFdc analysis conducted under the self-weight loading only,

the current internal stress resultants, \mathbf{p}_{curr} , need to be initialised once according to the presence of the self-weight loads of the beam elements as $\mathbf{p}_{curr} = \mathbf{p}_0$ (Equation 3.33) at the beginning of the global level iterations. Then, in the continuation of the EQFdc analysis for both self-weight and greenfield loading cases, the internal stress resultants need to be updated, \mathbf{p}_{up} (Equation 4.14) at each Gauss point level iteration as presented later in the chapter.

4.3 Element Level Iteration

The element level iteration is required for the flexibility analysis in the beam elements. To explain the determination of the global nodal internal forces for the beam elements, the force equilibrium between the external and internal forces is expressed separately for the beam elements in Equation (4.5). However, Equation (4.5) does not present an additional iteration procedure; in contrast, it is only represented in this way to highlight the vectors that correspond to the beam elements in Equation (4.1) as follows:

$$\mathbf{G}(\mathbf{U}_{ite,beams}) = \mathbf{F}_{EXT,beams} - \mathbf{F}_{INT,beams}(\mathbf{U}_{ite,beams}) \quad (4.5)$$

where $\mathbf{F}_{EXT,beams}$ is global nodal external forces applied to the beams, $\mathbf{F}_{INT,beams}$ is the global nodal internal forces associated with the beam elements and $\mathbf{U}_{ite,beams}$ is the global nodal displacement vector of the whole beam elements at a particular iteration (abbreviation of ‘ite’ refers to the global level iterations). $\mathbf{U}_{ite,beams}$ is incorporated as the external displacements in the flexibility analysis. Firstly, the reduced set of external displacements, $\mathbf{U}_{r,ext}$ need to be determined according to Equation (3.11) for the specified beam element in the flexibility analysis. To satisfy the compatibility between the reduced set of external, $\mathbf{U}_{r,ext}$ and internal displacements, $\mathbf{U}_{r,int}$ for the specified beam element, at a particular element level iteration (‘iteES’), the residual displacement vector is determined as $\mathbf{G}(\mathbf{P}_r^{iteES})$ for an estimate of a reduced set of forces, \mathbf{P}_r^{iteES} :

$$\mathbf{G}(\mathbf{P}_r^{iteES}) = \mathbf{U}_{r,int}(\mathbf{P}_r^{iteES}) - \mathbf{U}_{r,ext} \quad (4.6)$$

To find the internal forces that satisfy the compatibility between $\mathbf{U}_{r,int}$ and $\mathbf{U}_{r,ext}$, the following updates are needed for: the internal stress resultants, \mathbf{p} , the internal strain resultants, $\boldsymbol{\epsilon}$ and the reduced set of force vector, \mathbf{P}_r . The iteration procedure described in Section 4.4 is for the determination of internal stress and strain resultants at Gauss point level according to the element state determination (Spacone et al., 1996; Neuenhofer & Filippou, 1997). The element level updating procedure iterates until the compatibility between $\mathbf{U}_{r,ext}$ and $\mathbf{U}_{r,int}$ is reached (Equation 4.6). An iterative solution is required to find the suitable \mathbf{P}_r value by updating the incremental reduced set of forces, $\Delta\mathbf{P}_r$, at each iteration. According to the Newton-Raphson approach, $\mathbf{G}(\mathbf{P}_r)$ is linearised to get a better estimate of \mathbf{P}_r^{iteES} to give $\mathbf{P}_r = \mathbf{P}_r^{iteES}$ as:

$$\mathbf{G}(\mathbf{P}_r) \approx \mathbf{G}(\mathbf{P}_r^{iteES}) + \frac{\partial \mathbf{G}}{\partial \mathbf{P}_r} \Delta \mathbf{P}_r \quad (4.7)$$

where $\frac{\partial \mathbf{G}}{\partial \mathbf{P}_r}$ is the tangent flexibility matrix (Equation 3.25) and depends on the relationship between the internal stress and strain resultants for the specified material constitutive law (Sections 5.2 and 6.2).

$$\frac{\partial \mathbf{G}}{\partial \mathbf{P}_r} = \int_0^L \mathbf{b}^T \left(\frac{\partial \boldsymbol{\epsilon}}{\partial \mathbf{p}} \right) \mathbf{b} dx \quad (4.8)$$

By solving the following equation, incremental reduced set of forces, $\Delta\mathbf{P}_r$ is determined as:

$$\Delta \mathbf{P}_r = -\frac{\partial \mathbf{G}}{\partial \mathbf{P}_r} \mathbf{G}(\mathbf{P}_r^{iteES}) \quad (4.9)$$

Thus, the improved estimate of the reduced set of forces, $\mathbf{P}_r^{iteES+1}$, is computed as:

$$\mathbf{P}_r^{iteES+1} = \mathbf{P}_r^{iteES} + \Delta \mathbf{P}_r \quad (4.10)$$

The element state iterations continue until the residual displacements, \mathbf{G} reach a value less than the desired tolerance value ($tol = 10^{-3}$) of the magnitude of initial residual displacements, $\|\mathbf{G}(\mathbf{P}_r^1)\|$.

$$\|\mathbf{G}(\mathbf{P}_r^{iteES})\| < tol \times \|\mathbf{G}(\mathbf{P}_r^1)\| \quad (4.11)$$

When the compatibility between the reduced set of external and internal displacements is achieved for the specified beam element, the internal nodal force vector, \mathbf{P}_{beam} , needs to be calculated by using the rotation and reduced transformation matrices for the updated value of \mathbf{P}_r at the end of the element level iteration according to Equation (3.22). Then, the global internal nodal force vector of all beam elements, $\mathbf{F}_{INT,beams}$ is determined by assembling the \mathbf{P}_{beam} vector of each beam element.

$$\mathbf{F}_{INT,beams} = \mathbb{A}[\mathbf{P}_{beam}] \quad (4.12)$$

where \mathbb{A} is the assembly operator. If the EQFdc analysis is performed under the self-weight loading, then $\mathbf{F}_{INT,beams}$ needs to be determined according to Equation (3.37). For the EQFdc analysis performed under the greenfield displacement loading, only Equation (4.12) needs to be considered to determine $\mathbf{F}_{INT,beams}$. At the end of the element level iterations, the updated $\mathbf{F}_{INT,beams}$ are combined with the global internal force vectors of the stiffness formulations-based elements in the EQFdc model to compute the updated value of $\mathbf{F}_{INT}(\mathbf{U}_{ite})$ for the specified global nodal displacements, \mathbf{U}_{ite} . The updated $\mathbf{F}_{INT}(\mathbf{U}_{ite})$ is sent back into the global force equilibrium iterations and the analysis iterates until the global force equilibrium (Equation 4.1) is reached.

4.4 Gauss Point Level Iteration

The Gauss point level iteration is only employed for the fibre beam model to determine the

corresponding internal stress, $\mathbf{p}_{\text{fibre}}$ and strain, $\boldsymbol{\varepsilon}_{\text{fibre}}$ resultants of the fibre elements (Equation 3.32). The shear terms (V, γ) in Equation (3.32) are calculated without using an iterative solution. Firstly, the internal stress and strain resultants induced by $\Delta\mathbf{P}_r$ (determined from the element level iteration) need to be computed at each Gauss point along the beam length. The incremental internal stress resultants, $\Delta\mathbf{p}$, are computed as:

$$\Delta\mathbf{p} = \mathbf{b} \Delta\mathbf{P}_r \quad (4.13)$$

where \mathbf{b} is the force interpolation matrix given in Equation (3.19). Then, the current internal stress resultants in the beam, \mathbf{p}_{curr} , need to be updated (\mathbf{p}_{up}) with $\Delta\mathbf{p}$ as:

$$\mathbf{p}_{\text{up}} = \mathbf{p}_{\text{curr}} + \Delta\mathbf{p} \quad (4.14)$$

The incremental stress resultants, $\Delta\mathbf{p}$ applied to the beam create incremental strain resultants, $\Delta\boldsymbol{\varepsilon}$ at each Gauss point. To determine $\Delta\boldsymbol{\varepsilon}$, first, the local flexibility matrix, \mathbf{f} , needs to be computed. At the beginning of the EQFdc analysis, the local flexibility matrix is determined based on the linear elastic constitutive law for the beam's flexural and shear behaviour (Section 5.2). Later, the local flexibility matrix, \mathbf{f}_{up} is updated as $\mathbf{f}_{\text{up}} = \left(\frac{\partial\boldsymbol{\varepsilon}}{\partial\mathbf{p}}\right)$ at each Gauss level iteration according to the specified material constitutive laws (Section 6.2). Then, $\Delta\boldsymbol{\varepsilon}$ at each Gauss point is calculated and the current internal strain resultants, $\boldsymbol{\varepsilon}_{\text{curr}}$, are updated as $\boldsymbol{\varepsilon}_{\text{up}}$:

$$\Delta\boldsymbol{\varepsilon} = \mathbf{f}_{\text{up}} \Delta\mathbf{p} \quad (4.15)$$

$$\boldsymbol{\varepsilon}_{\text{up}} = \boldsymbol{\varepsilon}_{\text{curr}} + \Delta\boldsymbol{\varepsilon} \quad (4.16)$$

From this point, to determine the internal stress and strain resultants for the fibre beam model, the Gauss point level iteration procedure ('iteP' refers to the iteration number) is employed. The iterative solution based on the Newton-Raphson method is explained as follows:

- 1) Start the iteration process with the initial linear elastic estimate of the section stiffness of the fibre beam model, $\mathbf{k}_{\text{fibre}}$ (Equations 3.30 and 3.31). After the first iteration, $\mathbf{k}_{\text{fibre}}$ needs to be updated with the current values of $\left(\frac{d\sigma}{d\varepsilon}\right)_{\text{fibre}}$ determined from the fibre beam model based on the axial stress/strain constitutive relationship (Sections 5.2.1 and 6.2.1).
- 2) Estimate the incremental strain resultants for the fibre beam, $\Delta\varepsilon_{\text{fibre}}^{\text{iteP}}$ induced by the incremental stress resultants, $\Delta\mathbf{p}_{\text{fibre}}^{\text{iteP}}$ as:

$$\Delta\varepsilon_{\text{fibre}}^{\text{iteP}} = \mathbf{k}_{\text{fibre}}^{-1} \Delta\mathbf{p}_{\text{fibre}}^{\text{iteP}} \quad (4.17)$$

At the first estimate of the Gauss point level iterations, $\Delta\mathbf{p}_{\text{fibre}}^1$ is extracted as the fibre beam terms from Equation (4.13), where the first value of $\Delta\mathbf{P}_r^1$ is determined according to Equation (4.9).

- 3) Update the current internal strain resultants of the fibre beam, $\varepsilon_{\text{fibre}}^{\text{curr}}$ with $\Delta\varepsilon_{\text{fibre}}^{\text{iteP}}$ at each iteration to find the best estimate of updated $\varepsilon_{\text{fibre}}^{\text{up}}$ as:

$$\varepsilon_{\text{fibre}}^{\text{up}} = \varepsilon_{\text{fibre}}^{\text{curr}} + \Delta\varepsilon_{\text{fibre}}^{\text{iteP}} \quad (4.18)$$

- 4) Calculate the incremental axial strain of each fibre element, $\Delta\varepsilon_{\text{fibre}}^{\text{iteP}}$ using the values estimated in $\Delta\varepsilon_{\text{fibre}}^{\text{iteP}}$. Accordingly, the incremental axial strain for a fibre element, $\Delta\varepsilon_{\text{fibre}}^{\text{iteP}}$ in the cross-sectional area is:

$$\Delta\varepsilon_{\text{fibre}}^{\text{iteP}} = \Delta\varepsilon_c + y_{\text{fibre}}\Delta\kappa \quad (4.19)$$

where $\Delta\varepsilon_c$ is the incremental axial strain at the centre of the cross-section, $\Delta\kappa$ is the incremental curvature and y_{fibre} is the distance from the centroid of the cross-section to the centre of the fibre element (Figure 3.8).

- 5) Determine the axial stress in each fibre, σ_{fibre} , using $\Delta\varepsilon_{\text{fibre}}^{\text{iteP}}$ according to the

material constitutive law defined for the fibre beam elements (Sections 5.2.1 and 6.2.1).

- 6) Calculate the estimated values of axial force, N_{est} and the bending moment, M_{est} as the components of \mathbf{p}_{fibre} .
- 7) Find the residual internal force value, $\mathbf{G}(\Delta\boldsymbol{\varepsilon}^{iteP})$ between the applied element loads and the estimated values of N_{est} and M_{est} as:

$$\mathbf{G}(\Delta\boldsymbol{\varepsilon}^{iteP}) = \mathbf{p}_{applied} - \mathbf{p}_{fibre}(\Delta\boldsymbol{\varepsilon}^{iteP}) \quad (4.20)$$

where $\mathbf{p}_{applied}$ only includes the axial force and bending moment terms of \mathbf{p}_{up} in Equation (4.14) as $\mathbf{p}_{applied} = \mathbf{p}_{up}([1, 2])$. Accordingly, $\mathbf{p}_{fibre}(\Delta\boldsymbol{\varepsilon}^{iteP})$ is composed of the estimated values of the axial force and the bending moment as $\mathbf{p}_{fibre}(\Delta\boldsymbol{\varepsilon}^{iteP}) = [N_{est} \quad M_{est}]^T$.

- 8) Stop the Gauss point level iteration if:

$$\|\mathbf{G}(\Delta\boldsymbol{\varepsilon}^{iteP})\| < tol \quad (4.21)$$

where $\|\mathbf{G}(\Delta\boldsymbol{\varepsilon}^{iteP})\|$ is residual internal stress resultants and tol is the desired tolerance value (chosen as 10 N or 10 Nm). Otherwise, the incremental stress resultants vector for the fibre beam is updated as $\Delta\mathbf{p}_{fibre}^{iteP+1} = \mathbf{G}(\Delta\boldsymbol{\varepsilon}^{iteP})$ for the next cross-section level iteration and repeats the procedure from Step 2.

When the Gauss point level iteration is completed, the final value of $\boldsymbol{\varepsilon}_{fibre} = \boldsymbol{\varepsilon}_{fibre}^{up}$ is placed into Equation (3.32). After that, the shear strain, γ and the shear term of $\mathbf{k}_{section}$ matrix need to be calculated according to the material constitutive models defined for the beam shear behaviour (Sections 5.2.2 and 6.2.2).

When the internal strain resultants are determined at each Gauss point, it is convenient to calculate the reduced set of internal displacements, $\mathbf{U}_{r,int}$ as:

$$\mathbf{U}_{r,int} = \int_0^L \mathbf{b}^T \boldsymbol{\varepsilon} dx = \int_0^L \mathbf{b}^T \begin{bmatrix} \boldsymbol{\varepsilon}_{fibre} \\ \gamma \end{bmatrix} dx \quad (4.22)$$

The updated $\mathbf{U}_{r,int}$ returns to the element level iteration to be used in the compatibility check in Equation (4.6).

4.5 Conclusion

The general solution procedures employed for the EQFdc analysis comprise three main iterations in global, element and Gauss point levels. The global level iterations are performed for the whole structure. In addition to the global level iterations, the flexibility formulations-based beam elements also require element and Gauss point level iterations to conduct the flexibility analysis before they are incorporated with the whole structure. To solve the flexibility analysis, the Newton-Raphson method is chosen for the element and Gauss point level iterations. In contrast, the Modified Newton-Raphson method is considered for the stiffness formulation-based global level iteration.